TECHNISCHE UNIVERSITÄT DRESDEN

Validation of polarized simulations for WZjj production in Sherpa

Bachelor-Arbeit
zur Erlangung des Hochschulgrades
Bachelor of Science
im Bachelor-Studiengang Physik

vorgelegt von

Tim Burghardt
geboren am 23.01.2001 in Dresden

Institut für Kern- und Teilchenphysik
Fakultät Physik
Bereich Mathematik und Naturwissenschaften
Technische Universität Dresden
2022

Eingereicht am 27. Dezember 2022

1. Gutachter: Dr. Frank Siegert
2. Gutachter: Prof. Dr. Dominik Stöckinger

Summary

Abstract
Englisch
The process of Vector Boson Scattering of two longitudinally polarized vector bosons is deeply linked to the relationship of gauge invariance and the mechanism of electroweak symmetry breaking, since without a Higgs boson, the predicted cross section would violate unitarity. At the current version of SHERPA 2.2.13, SHERPA is not capable of simulating the polarization of vector bosons. However, a currently unpublished version of SHERPA can be used to generate these processes in the future. For the fully leptonic WZ channel, polarized samples are generated and compared with reference data for a center of mass energy $\sqrt{s} = 13\,\text{TeV}$. Considering the total cross sections as well as the distributions of the differential cross sections, a good agreement is achieved. Furthermore, the generated events are compared with official Atlas Monte Carlo samples generated with MADGRAPH .

Abstract
Deutsch
Die Streuung zweier longitudinal polarisierter Vektorbosonen ist tief mit der Eichinvarianz und dem Mechanismus der elektroschwachen Symmetriebrechung verknüpft, da der vorhergesagte Wirkungsquerschnitt ohne die Existenz eines Higgs Bosons die Unitarität verletzen würde. In der aktuellen Version von SHERPA 2.2.13 kann SHERPA keine Polarisation von Vektorbosonen simulieren. Jedoch wird dies mit einer noch nicht veröffentlichten Version in Zukunft möglich sein. Für den vollständig leptonischen WZ Kanal werden polarisierte Vektorbosonen bei einer Schwerpunktsenergie von $\sqrt{s} = 13\,\text{TeV}$ generiert und die Daten werden mit Literaturwerten verglichen. Für die totalen Wirkungsquerschnitte sowie für die Verteilungen der differentiellen Wirkungsquerschnitte wurden gute Übereinstimmungen erzielt. Des Weiteren wurden die generierten Daten mit offiziellen Atlas Monte Carlo Daten, welche mit MADGRAPH generiert wurden, verglichen.

Contents

1 Introduction

Physics can be considered as one of the fundamental natural sciences with its main destination being nothing short of getting a deep understanding on how the universe works. The progress in physics over the past decades led to new discoveries in solid-state physics, quantum mechanics and nuclear physics, which play a huge role as new technologies advance to benefit humanity. Particle physics deals with the fundamental constituents of our nature, the elementary particles and their interactions. Our current knowledge about these particles and the forces between them is expressed in the Standard Model of particle physics (SM), which illustrates one of the biggest triumphs of leading-edge particle physics. The discovery of the Higgs boson at the Large Hadron Collider (LHC) at CERN in 2012 [21, 20] underlines the success of the Standard model, since now all of the particles predicted by the SM have been observed. However, there are still some open questions in modern physics like the existence of dark matter and dark energy [22] which provide evidence that the SM is not the ultimate theory and that there might be physics beyond the Standard model. Further examples are the search for supersymmetric particles [3] or theories that unify the different forces we observe today.

The LHC [16] plays an important role in nowadays physics, since these high energy scales can be used to investigate the properties of the fundamental particles and probe the predictions of the SM. One of the predictions of the SM is the scattering of polarized vector bosons like the gauge bosons from the electroweak interaction. This process of vector boson Scattering (VBS) of longitudinally polarized W and Z bosons is directly linked to the mechanism of electroweak symmetry breaking (EWSB) [15] as it tests the SM innermost gauge symmetry structure. In Run 2 at the LHC with a center of mass energy of 13 TeV, ATLAS and CMS were able to provide evidence that vector boson scattering actually occurs [18]. The polarization of vector bosons at the LHC has been investigated in many different studies, like [4, 24, 26, 19, 9].

In this thesis polarized VBS will be studied in the electroweak $WZjj$ process with an electron-positron pair, a muon and muon neutrino as well as two jets in the final state. Although the cross section of the WZ channel is larger than the one for the ZZ channel, the presence of a leptonically decaying W boson does not allow for the complete reconstruction of the momentum of the neutrino. The Monte Carlo event generator Sherpa is used to generate samples that include information about the polarization of the vector bosons.

First, in chapter 2 a short introduction to the Standard Model and the mechanism of Electroweak Symmetry Breaking as well as an overview about the process of VBS and the functionality of Monte Carlo event generators is given. Chapter 3 deals with the question how polarized samples can be generated in Sherpa and explains the setup of the simulation. The generated events are studied in chapter 4. In chapter 5 a short comparison between the event generators Sherpa and MadGraph is performed. Lastly a summary and outlook is given in chapter 6.

2 Theoretical Background

In this chapter, a short introduction and overview of the underlying theory behind the investigated process is presented. A similar approach as in [9, 26, 19, 13, 27, 1] is used.

2.1 The Standard Model and Electroweak Symmetry Breaking

The fundamental constituents of our nature, namely the elementary particles and the forces, the interactions between the particles, are described by the Standard Model of particle physics (SM). Currently, the SM describes the electromagnetic, strong and weak interactions. The fourth force, gravity, can not be described by the SM, since their impact on particle processes at achievable energy scales is negligible.
The SM is a renormalizable quantum field theory based on local gauge symmmetry $SU(3)_C \otimes SU(2)_L \otimes U(1)_Y$, leading to a large set of conserved charges and currents. These charges are the electric charge, the weak isospin for the weak force and the color charge for the strong interaction. The strong interaction can be derived from the $SU(3)$ group, the remaining $SU(2) \otimes U(1)$ group combines the weak and electromagnetic interaction and is therefore referred to as the electroweak interaction.

There are two major group of particles, first the fermions. All fermions are spin-1/2-particles and can be divided further into the quarks, which are the constituents of protons and neutrons and carry color and electro-weak charges, and the leptons, which are the electron e^-, muon μ^-, tauon τ^- and three associated neutrinos ν_e, ν_μ and ν_τ, who only carry electro-weak charges. These matter fermions come in three different generations, with different masses but identical quantum numbers. In addition to that, every fermion has a dedicated antiparticle that has the same mass, but opposite physical charges.
The particles who exchange the fundamental interactions between the fermions are called bosons and have spin 1. These force carriers are the photon γ for the electromagnetic interaction, the gauge bosons $W^\pm$ and Z for the weak interaction and the eight gluons g for the strong force. Since they are all spin-1-particles, they are also called vector bosons. The last boson is the Higgs boson H. This is the only boson that has spin 0 and is therefore called a scalar boson. The photon and the gluons are massless, due to the conservation of the corresponding symmetry generators, namely the electric and the color charges. Given that the gauge bosons

$W^{\pm}$ and Z have relatively large masses, this indicates that the corresponding symmetries are broken. In the SM, the Higgs mechanism is responsible for the electroweak symmetry breaking which is now discussed briefly.

The Weinberg-Salam model is a $SU(2)_L \otimes U(1)_Y$ gauge theory and describes the electroweak interactions. It contains one $U(1)_Y$ gauge boson B_μ and three $SU(2)_L$ gauge bosons W^i_μ, $i = 1, 2, 3$. For the kinetic energy term follows

$$\begin{aligned} \mathcal{L}_{\text{KE}} &= -\frac{1}{4} W^i_{\mu\nu} W^{\mu\nu i} - \frac{1}{4} B_{\mu\nu} B^{\mu\nu}, \\ W^i_{\mu\nu} &= \partial_\nu W^i_\mu - \partial_\mu W^i_\nu + g\epsilon^{ijk} W^j_\mu W^k_\nu, \\ B_{\mu\nu} &= \partial_\nu B_\mu - \partial_\mu B_\nu. \end{aligned} \tag{2.1}$$

To couple to the gauge fields, a complex scalar $SU(2)$ doublet Φ is introduced

$$\Phi = \begin{pmatrix} \phi^+ \\ \phi^0 \end{pmatrix} \tag{2.2}$$

and the scalar potential can be expressed by

$$V(\Phi) = \mu^2 |\Phi^\dagger \Phi| + \lambda \big(|\Phi^\dagger \Phi|\big)^2 \tag{2.3}$$

where $\lambda > 0$. If $\mu^2 < 0$, $\Phi = 0$ is not the state of minimum energy and the field develops a vacuum expectation value (VEV). Since the potential only depends on the combination $\Phi^\dagger\Phi$, one minima can be chosen arbitrarily

$$\langle \Phi \rangle = \frac{1}{\sqrt{2}} \begin{pmatrix} 0 \\ v \end{pmatrix} \tag{2.4}$$

with $v = \sqrt{-\frac{\mu^2}{\lambda}}$. The scalar doublet has hypercharge $Y = 1$ and the electromagnetic charge counts $Q = \frac{Y}{2} + I^{(3)}_W$. Hence $Q\langle\Phi\rangle = 0$, the scalar VEV does not lead to a break of electromagnetism. But this VEV then breaks the $SU(2)_L \otimes U(1)_Y$ symmetry. Due to contributions of the scalar doublet, the Lagrangian has to be extended

$$\mathcal{L}_{\text{s}} = (D_\mu \Phi)^\dagger (D^\mu \Phi) - V(\Phi), \tag{2.5}$$

$$D_\mu = \partial_\mu + igT \cdot W_\mu + i\frac{g'}{2} B_\mu Y \tag{2.6}$$

where $T = \frac{1}{2}\sigma$ are the three generators of the $SU(2)$ symmetry (Pauli matrices). Since no Goldstone bosons occur in unitary gauge and only the Higgs scalar remains after the symmetry breaking, the scalar doublet now reads in unitary gauge

$$\Phi = \frac{1}{\sqrt{2}} \begin{pmatrix} 0 \\ v+h \end{pmatrix} \tag{2.7}$$

Using the kinetic energy term in (2.5) leads to

$$\frac{1}{2}(0,v)\left(\frac{1}{2}g\sigma\cdot W_\mu + \frac{1}{2}g'B_\mu\right)^2 \begin{pmatrix} 0 \\ v \end{pmatrix} \tag{2.8}$$

The physical gauge fields are then made up of two neutral fields Z_μ and A_μ and two charged fields $W^\pm$:

$$\begin{aligned} W^\pm_\mu &= \frac{1}{\sqrt{2}}(W^1_\mu \mp iW^2_\mu) \\ Z_\mu &= \frac{-g'B_\mu + gW^3_\mu}{\sqrt{g^2+g'^2}} \\ A_\mu &= \frac{gB_\mu + g'W^3_\mu}{\sqrt{g^2+g'^2}} \end{aligned} \tag{2.9}$$

In the Lagrangian, the term $(D_\mu\Phi)^\dagger(D^\mu\Phi)$ is responsible for the generation of the masses of the gauge bosons. This term now becomes

$$\begin{aligned} (D_\mu\Phi)^\dagger(D^\mu\Phi) = \frac{1}{2}(\partial_\mu h)(\partial^\mu h) &+ \frac{1}{8}g^2(W^1_\mu + iW^2_\mu)(W^{1\mu} - iW^{2\mu})(v+h)^2 \\ &+ \frac{1}{8}(gW^3_\mu - g'B_\mu)(gW^{3\mu} - g'B^\mu)(v+h)^2 \end{aligned} \tag{2.10}$$

Since the masses of the gauge bosons are determined only by the terms that are quadratic in the gauge boson fields, the masses can be identified to be:

$$\begin{aligned} m_{\mathrm{W}} &= \frac{1}{2}gv \\ m_{\mathrm{Z}} &= \frac{1}{2}v\sqrt{g^2+g'^2} \\ m_{\mathrm{A}} &= 0 \end{aligned} \tag{2.11}$$

Before the spontaneous symmetry breaking has occurred, we had 12 degrees of freedom: four degrees of freedom from the complex scalar $SU(2)_L$ doublet Φ, six from the massless $SU(2)_L$ gauge field W_i and 2 from a massless $U(1)_Y$ gauge field B. After the symmetry breaking we get 1 degree of freedom from a real scalar field h, 9 from the massive W and Z fields and 2 from a massless photon. The scalar degrees of freedom were "sacrificed" to give the $W^\pm$ and Z bosons their longitudinal components.

Equation (2.10) also contains terms of order HVV and $HHVV$, where $V = W^\pm, Z$ which

correspond to a triple and a quartic vertex for the interaction between the gauge bosons and the Higgs boson.
By applying another gauge than unitary gauge, this will indeed lead to Goldstone bosons in the spectrum and the scalar field is modified

$$\Phi = \frac{1}{\sqrt{2}} e^{i\frac{\omega \cdot \sigma}{2v}} \begin{pmatrix} 0 \\ v+h \end{pmatrix} \tag{2.12}$$

Three Goldstone bosons appear in the Standard Model, $\vec{\omega} = (\omega^{\pm}, z)$.
Until now, no fermions have been included in this theory. They can be expressed by their left- and right-handed projections

$$\psi_{\mathrm{L,R}} = \frac{1}{2}(1 \mp \gamma_5)\psi \tag{2.13}$$

where γ_5 is the fifth Dirac matrix. Due to the fact, that the W boson only couples to left-handed fermions, the $SU(2)_L$ doublet can be denoted as

$$L_L = \begin{pmatrix} \nu_{eL} \\ e_L \end{pmatrix} \tag{2.14}$$

for leptons of the first generation. The hypercharge for left-handed leptons must be $Y_L = -1$. The neutrino has only one helicity state ν_L, since neutrinos are massless. Given that right-handed fields do not interact with W bosons, the right-handed electron has to be an $SU(2)_L$ singlet, e_R, with a hypercharge of $Y_{e_R} = -2$. The notation for leptons from other generations is equivalent.
The Higgs mechanism generates the masses of the W and Z bosons, but also can be used to generate the masses of fermions. A fermion mass term of the form

$$-m\bar{\psi}\psi = -m(\bar{\psi}_L\psi_R + \bar{\psi}_R + \psi_L \tag{2.15}$$

violates the $SU(2)_L \otimes U(1)_Y$ gauge symmetry because left- and right-handed chiral states transform differently. Gauge invariant mass terms can be formed for all Dirac fermions from

$$\mathcal{L} = -g_{\mathrm{f}}\left[\bar{L}\phi R + (\bar{L}\phi R)^{\dagger}\right] \quad \text{or} \quad \mathcal{L} = g_{\mathrm{f}}\left[\bar{L}\phi_{\mathrm{c}} R + (\bar{L}\phi_{\mathrm{c}} R)^{\dagger}\right], \tag{2.16}$$

where g_{f} denotes the Yukawa coupling, ϕ_{c} the conjugate doublet, L the $SU(2)$ doublets for left-handed chiral fermions and R the $SU(2)$ singlets for right-handed chiral fermions. The fermion masses can be obtained from the relationship

$$g_{\mathrm{f}} = \sqrt{2}\frac{m_{\mathrm{f}}}{v} \tag{2.17}$$

with the vacuum expectation value of the Higgs field $v = 246\,\mathrm{GeV}$.

2.2 Polarization

In general, polarization describes the degree to which the spin of a particle is aligned with the direction of the particle's momentum. This can be quantified using the helicity h:

$$h = \frac{\vec{S} \cdot \vec{p}}{|\vec{p}|} \tag{2.18}$$

which specifies the projection of the spin S onto the direction of the momentum of the particle $\vec{p}$. In quantum mechanics, the angular momentum and thereby the helicity is quantized. For a massive particle of spin S, the helicity has $2S+1$ possible eigenvalues reaching from $-S, -S+1, \ldots, 0, \ldots, S$ for particles whose spin is an integer and from $-S, -S+1, \ldots, -1/2, +1/2, \ldots, S$ if the particle's spin has a half-integer value. For $W^{\pm}$ and Z bosons the possible eigenvalues for h are:

- $h = 0$: longitudinal polarization
- $h = \pm 1$: transverse polarization

since both bosons have spin 1. Longitudinal polarization implies that the spin and the direction of the momentum are orthogonal, while for a helicity of ± 1 the direction of a particle's spin is either the same as the direction of its momentum or opposite. A helicity of 1 is also called right-handed polarization while $h = -1$ is referred to as left-handed polarization.
By definition, the helicity of a particle is not Lorentz invariant, since a boost in a system which travels faster than the particle is always possible and thus the helicity changes sign. For massless particles however, the helicity becomes Loretz invariant as massless particles travel at the speed of light and then the only two possible eigenvalues for the helicity are $\pm S$.

2.3 Vector Boson Scattering

The process of vector boson scattering (VBS) is one of the rarest processes we can currently measure experimentally, as the cross section predicted by the standard model is quite small. Due to the short lifetime of vector bosons, they can not be observed directly and thus VBS processes can only be accessed as a subprocess of more complicated reactions, which contain the radiation of $W^{\pm}$ or Z bosons from quarks in the initial state. Subsequently the bosons scatter and decay either leptonically into leptons or hadronically into quarks. The initial state quarks can be seen from the detector as jets in the final state. They only interact via weak interactions, which implies that they are barely deflected and thus have a high invariant mass and a tight angular separation. This yields to a reasonable separation of signal and background although the cross section is very small. A visualization of the $W^{\pm}Z$ scattering process as it happens at the LHC is shown in Figure 2.1. As described in section 2.1 the SM not only gives

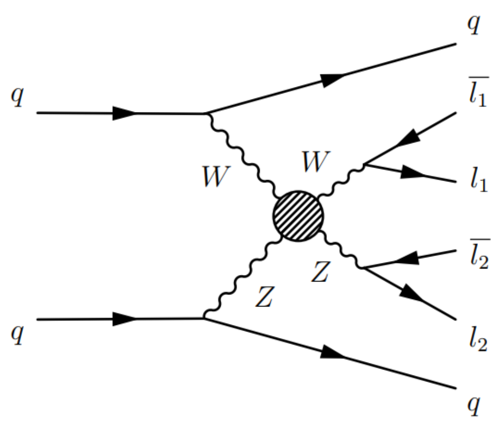

Figure 2.1: Feynman diagram for $W^{\pm}Z$ scattering

rise to the scattering between vector bosons, but also predicts triple and quartic couplings between the gauge bosons and one or two Higgs bosons. The diagrams contributing to VBS can be seen in Figure 2.2. These include two diagrams with a triple vertex, one with a quartic vertex and one with the important Higgs boson. The coupling order of this specific VBS

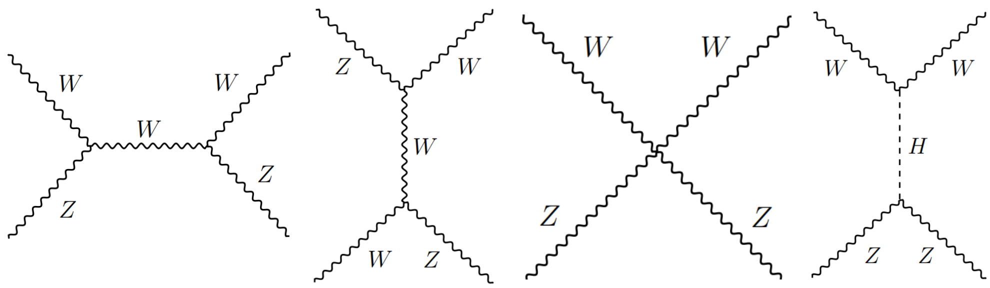

Figure 2.2: Feynman diagrams contributing to $W^{\pm}Z$ scattering

process as shown in Figure 2.1 is $\mathcal{O}(\alpha_{\mathrm{EW}}^6)$. Since we can only measure particles in the final state, there is a variety of diagrams that have the same final state particles but do not follow the typical scheme of vector boson scattering. Dropping such non-resonant and single-Z-resonant or single-$W^{\pm}$-resonant diagrams may violate gauge invariance. Therefore other diagrams have to be taken into account when dealing with VBS. Some of these diagrams are displayed in Figure 2.3. The diagram on the left depicts a non-resonant process, the other two show single-resonant contributions. Another constraint is applied by discarding processes containing b quarks in the initial- or final state. Processes involving b quarks in the initial state lead to a top quark resonance, shown in Figure 2.4, where no VBS happens. The contribution of these processes to the final cross section can not be neglected, and thus they have to be restricted. Finally, also diagrams of the order $\mathcal{O}(\alpha_{\mathrm{EW}}^4\alpha_{\mathrm{s}}^2)$ can have the same final state particles, but in this thesis, only the process of order $\mathcal{O}(\alpha_{\mathrm{EW}}^6)$ is investigated.

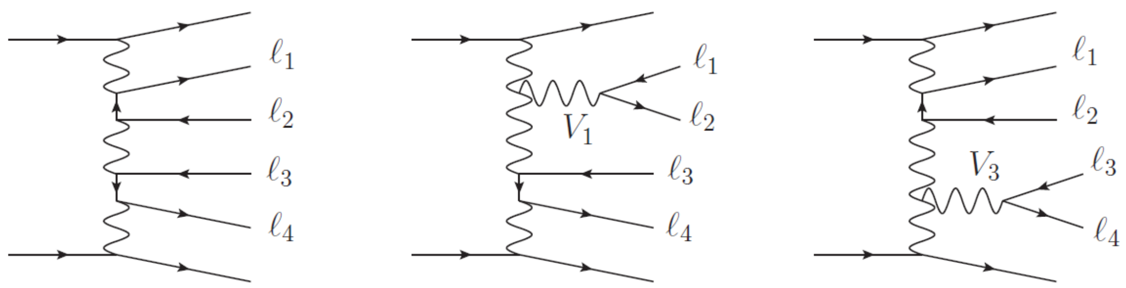

Figure 2.3: Examples of non-resonant and single-resonant Feynman diagrams for VBS at the LHC [5]

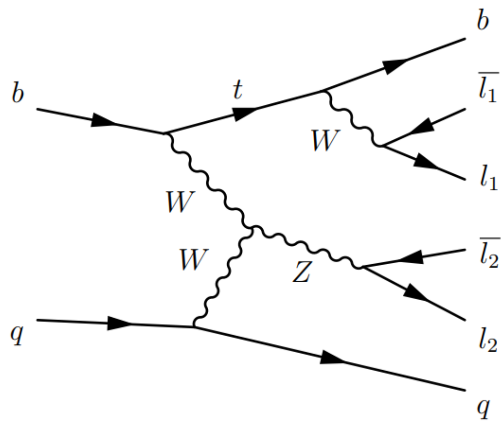

Figure 2.4: t channel Feynman diagram of the tZj production process

As described in section 2.1 the vector boson scattering of $W^{\pm}Z$ is profoundly connected to the mechanism of EWSB. Three Goldstone bosons are required, so that $W^{\pm}$ and Z bosons receive their longitudinal polarization components. Therefore, the scattering process of two longitudinally polarized bosons $W^{\pm}_{\mathrm{L}}Z_{\mathrm{L}} \rightarrow W^{\pm}_{\mathrm{L}}Z_{\mathrm{L}}$ is interesting to study, since without any Higgs boson contributions, this process would violate unitarity. However, this break of unitarity does not occur when only considering transverse polarized vector bosons, independent of contributions from the Higgs bososn.

Given that only final state particles can be observed, it is necessary to use sensitive observables to infer about the polarization information of the vector bosons. One variable that can be used to analyze the behaviour for different polarizations is the cosine of the decay angle θ. For leptonically decaying W^+ bosons, the angle θ is computed in the rest frame of the W^+ boson between the charged lepton and the direction of the W^+ boson's momentum in the laboratory frame. Similarly for decaying Z bosons, the lepton is substituted with the negatively charged lepton. With that definition, every polarization is now associated with a particular distribution of the decay angle of the lepton. The expected distributions for the decay angle θ for a polarized W^+ and Z boson are shown in Figure 2.5

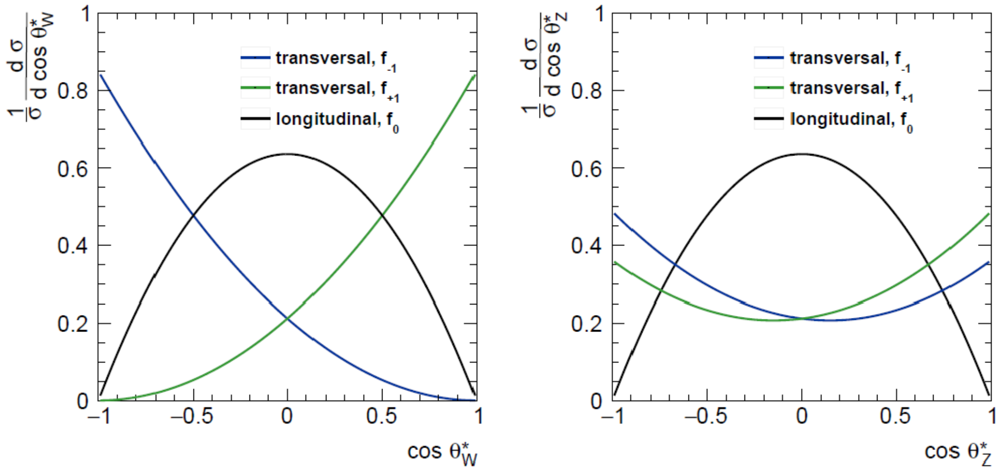

Figure 2.5: Normalized distribution of the decay angle for different polarizations for a W^+ boson (left) and for a Z boson (right) [9]

2.4 Monte Carlo Event Generators

In the final state of high energy particle collisions like the ones at the Large Hadron Collider (LHC), a large amount of particles are produced. To simulate events that are comparable with the measured data at the LHC, a huge amount of effort has to be made. Programs that are designed to generate events like they take place during proton proton collisions at the LHC are called general-purpose Monte Carlo (MC) event generators. Since the underlying physics of proton proton collisions is quite complex, only a short introduction to MC event generators is given. Further information can be found in [11].

First of all, the events that correspond to the hard scattering subprocess are generated. The relevant matrix elements are calculated only for a given order of pertubation theory and after that, the phase space integral is computed by using Monte Carlo methods to deal with the large amount of possible dimensions. Since at proton accelerators like the LHC, each parton inside a proton only holds a small fraction of the entire momentum of the proton, parton density functions (PDFs) are introduced which are based on fits to measured data.

The next step includes the simulation of parton showers and hadronization effects. Unstable particles decay and stable hadrons are formed. In addition to that, bremsstrahlung and further pertubative effects have to be considered. To get a reasonable comparison with measured data, further detector effects like underlying events and multi-parton interactions as well as initial state and photon radiation have to be taken into account. As a final step, the response of the detector has to be simulated, where for example the material composition and geometry of the detector play an important role. From now on the simulated events are described by the amount of energy that is deposited in the different parts of the detector. There is a variety of different MC event generators that can be used for the simulation of events. In this thesis, SHERPA [10] is employed.

3 Setup of the Simulation

Monte-Carlo generators are used to provide proper simulations of the processes as they happen during proton collisions at the LHC. Therefore, this chapter describes the different steps that are executed to generate polarized events with the Monte-Carlo event generator Sherpa.

3.1 Simulation of Polarized Events with Sherpa

To analyze the polarized W^+Z vector boson scattering channel, a development version of Sherpa 3.0.0 [25] is used for simulating samples that include polarization information of the vector bosons, since the current version of Sherpa [10] can not deal with it. In this thesis, all simulations have been performed at parton level and leading order. The following process is investigated for LHC run 2 settings at a center of mass energy of 13 TeV:

$$pp \to e^+e^-\mu^+\nu_\mu\, jj \tag{3.1}$$

Furthermore, only tree level electroweak contributions are considered ($\mathcal{O}(\alpha_{\mathrm{EW}}^6)$) and partonic processes which involve b quarks are neglected. To get results that can be compared with [5], the following cuts are applied:

Kinematic cuts on the jet system

- transverse momentum: $p_{\mathrm{T}}^{\mathrm{j}} > 20\,\mathrm{GeV}$;
- rapidity: $|\eta^{\mathrm{j}}| < 5$;
- invariant mass of the two jets: $M_{\mathrm{jj}} > 500\,\mathrm{GeV}$;
- rapidity separation between the two jets: $|\Delta\eta_{\mathrm{jj}}| > 2.5$;

Kinematic cuts on the charged leptons

- transverse momentum: $p_{\mathrm{T}}^{\mathrm{l}} > 20\,\mathrm{GeV}$;
- rapidity: $|\eta^{\mathrm{l}}| < 2.5$;

Further cuts

- invariant mass of the four leptons: $M_{\mathrm{WZ}} > 200\,\mathrm{GeV}$;

- difference between pole mass of the Z boson and invariant mass of the e^+e^- pair: $|M_{e^+e^-} - M_Z| < 15\,\text{GeV}$;
- missing transverse momentum: $p_T^{\text{miss}} > 40\,\text{GeV}$;

The M_{WZ} cut is applied after neutrino reconstruction. A cut on the invariant mass of the lepton pair and the Z pole mass is necessary to reduce γ contributions in the amplitudes and to allow for the separation of resonant diagrams. The renormalization and factorization scale are set to $\mu = M_{4l}/\sqrt{2}$ and `NPDF30_lo_as_0130` PDFs [12] are used.

Two different types of samples are produced, first the full sample where only the particles in the initial and final state are declared. The SHERPA run card can be found in section A.2. To simulate polarized samples for W^+ and Z bosons, the SHERPA run card had to be adapted and is also displayed in section A.2. The `PROCESSES` and `HARD_DECAYS` part of the data card has to be modified, since now vector bosons are produced directly, which is described in the `PROCESSES` method. Afterwards they decay as declared in the `HARD_DECAYS` definition. In `PARTICLE_DATA` the `Width` of the intermediate vector bosons has to be set to zero, due to the fact that they are treated as stable particles. Per default, the vector boson polarization is defined in the laboratory frame, which is also used in this thesis. For the full sample the

$$\begin{array}{ll} \text{full:} & pp \to e^+e^-\mu^+\nu_\mu\, jj \\ \text{polarized:} & pp \to W^+_{\text{L,T}}\, Z_{\text{L,T}}\, jj \to e^+e^-\mu^+\nu_\mu\, jj \end{array}$$

generator level cuts are applied which are described above. Since for the polarized sample the leptons are not part of the `PROCESSES` definition, the cuts are applied in the analysis after the SHERPA run. SHERPA is capable of simulating all polarized cross sections in one simulation run, meaning simulations for transverse and longitudinal vector bosons as well as unpolarized samples, where no specific polarization information is given. In the following a short overview is presented on how to define polarization for particles in intermediate states [17].

Since vector bosons like $W^\pm$ and Z are intermediate particles described by propagators, defining polarization for vector bosons is not trivial. The propagator term can be rewritten by applying the completeness relation

$$\left(-g^{\mu\nu} + \frac{q^\mu q^\nu}{m_V^2}\right) = \sum_{\lambda=1}^{4} \epsilon^\mu_\lambda(q)\epsilon^{*\nu}_\lambda(q). \tag{3.2}$$

The fourth polarization does not contribute and vanishes if the decay fermions are massless. A helicity basis for the polarization vectors $\epsilon^\mu_i(q)$ is given by [14]

$$\begin{aligned} \epsilon^\mu_\pm(q) &= \frac{e^{\mp i\phi}}{\sqrt{2}}\left(0, -\cos\theta\cos\phi \pm i\sin\phi, -\cos\theta\sin\phi \mp i\cos\phi, \sin\theta\right), \\ \epsilon^\mu_0(q) &= \frac{q^0}{m}\left(\frac{|\vec{q}|}{q^0}, \cos\phi\sin\theta, \sin\phi\sin\theta, \cos\theta\right) \end{aligned} \tag{3.3}$$

A definition of polarization is only possible if the matrix element factorizes in production and decay. For a single W production and decay, this becomes

$$\mathcal{M} = \mathcal{M}_{\mu}^{\text{prod}} \left(\frac{i\left(-g^{\mu\nu} + \frac{q^{\mu}q^{\nu}}{m_W^2}\right)}{q^2 - m_W^2 + i\Gamma_W m_W} \right) \mathcal{M}_{\nu}^{\text{decay}} \tag{3.4}$$

For non-resonant contribution,s no factorization in production and decay is possible and hence no definition of polarization is feasible. Thus approximations are necessary. Sherpa uses the so called narrow-width-approximation (NWA) [6]

$$\frac{1}{\left(q^2 - m_W^2\right)^2 + \Gamma_W^2 m_W^2} \to \frac{\pi\delta(q^2 - m_V^2}{\Gamma_V m_V} \tag{3.5}$$

The matrix element in (3.4) simplifies and leads to

$$\mathcal{M} = \frac{\pi}{\Gamma_W m_W} \sum_{\lambda=1}^{3} \mathcal{M}_{\mu}^{\text{prod}} \epsilon_{\lambda}^{*\mu} \epsilon_{\lambda}^{\nu} \mathcal{M}_{\nu}^{\text{decay}} = \frac{\pi}{\Gamma_W m_W} \sum_{\lambda=1}^{3} \mathcal{M}_{\lambda}^{\mathcal{P}} \mathcal{M}_{\lambda}^{\mathcal{D}} := \sum_{\lambda=1}^{3} \mathcal{M}_{\lambda}^{\mathcal{F}} \tag{3.6}$$

where $\mathcal{M}_{\lambda}^{\mathcal{F}}$ denotes the amplitude with a single polarization for an intermediate vector boson. For the cross section σ we get

$$\sigma \propto |\mathcal{M}|^2 = \underbrace{\sum_{\lambda} \left|\mathcal{M}_{\lambda}^{\mathcal{F}}\right|^2}_{\substack{\text{polarized cross section} \\ \text{for VB helicity } \lambda}} + \underbrace{\sum_{\lambda, \lambda'} \mathcal{M}_{\lambda}^{\mathcal{F}*} \mathcal{M}_{\lambda'}^{\mathcal{F}}}_{\text{interference terms}} . \tag{3.7}$$

In general the interference terms in (3.7) are not equal to zero and only vanish when the integration is performed over the full range of the angle ϕ. In practice, cuts on the charged leptons and on the transverse missing momentum are applied and thus prevent from full integration.

3.2 Neutrino reconstruction

Due to the fact, that the Large Hadron Collider (LHC) at CERN can not detect neutrinos, since they only interact via the weak force and therefore the energy deposited in the detector material is neglectable, their is always a mismatch in the transverse momentum which is called missing transverse momentum $p_{\text{T}}^{\text{miss}}$. In processes involving vector boson scattering like W^+Z this missing momentum can be used to reconstruct the transverse momentum of the neutrino. However, the full momentum of the neutrino can not be reconstructed, since the total momentum of an event along the z axis, which points along the beam axis, is not known.

If the missing transverse momentum is identified with the transverse momentum of the neutrino, only the z-component of the neutrino's momentum is unknown. This can be computed by setting the invariant mass of the $l^+\nu_\mathrm{l}$ system to be equal to the pole mass of the W boson.

$$p_\mu p^\mu = M_\mathrm{W}^2 = \begin{pmatrix} E^\mathrm{l} + E^\nu \\ p_x^\mathrm{l} + p_x^\nu \\ p_y^\mathrm{l} + p_y^\nu \\ p_z^\mathrm{l} + p_z^\nu \end{pmatrix} \cdot \begin{pmatrix} E^\mathrm{l} + E^\nu \\ -(p_x^\mathrm{l} + p_x^\nu) \\ -(p_y^\mathrm{l} + p_y^\nu) \\ -(p_z^\mathrm{l} + p_z^\nu) \end{pmatrix} \tag{3.8}$$

$$= (E^\mathrm{l} + E^\nu)^2 - (p_x^\mathrm{l} + p_x^\nu)^2 - (p_y^\mathrm{l} + p_y^\nu)^2 - (p_z^\mathrm{l} + p_z^\nu)^2 \tag{3.9}$$

$$= E^{\mathrm{l}2} + 2E^\mathrm{l}E^\nu + E^{\nu 2} - {p_x^\mathrm{l}}^2 - 2p_x^\mathrm{l}p_x^\nu - p_x^{\nu 2} - {p_y^\mathrm{l}}^2 - 2p_y^\mathrm{l}p_y^\nu - p_y^{\nu 2} - {p_z^\mathrm{l}}^2 - 2p_z^\mathrm{l}p_z^\nu - p_z^{\nu 2} \tag{3.10}$$

Since the mass of the lepton is relatively small compared to the mass of the W Boson, the term $E^{\mathrm{l}2} - {p_\mathrm{T}^\mathrm{l}}^2 - {p_z^\mathrm{l}}^2$ can be neglected. With the introduction of the transverse momentum vector of the lepton $\vec{p_\mathrm{T}}^\mathrm{l}$ and neutrino $\vec{p_\mathrm{T}}^\nu$, the fact that the neutrino is massless and therefore $E^{\nu 2} = \vec{p}^\nu$, the expression can be simplified:

$$\implies 2E^\mathrm{l}E^\nu = 2p_z^\mathrm{l}p_z^\mathrm{l} + 2\vec{p_\mathrm{T}}^\mathrm{l} \cdot \vec{p_\mathrm{T}}^\nu + M_\mathrm{W}^2 \tag{3.11}$$

$$= 2p_z^\mathrm{l}p_z^\nu + 2\delta\ , \qquad \delta = \frac{M_\mathrm{W}^2}{2} + \vec{p_\mathrm{T}}^\mathrm{l} \cdot \vec{p_\mathrm{T}}^\nu \tag{3.12}$$

$$\implies E^{\nu 2} = {p_\mathrm{T}^\nu}^2 + p_z^{\nu 2} = \frac{{p_z^\mathrm{l}}^2 p_z^{\nu 2} + \delta^2 + 2p_z^\mathrm{l}p_z^\nu\delta}{E^{\mathrm{l}2}} \tag{3.13}$$

$$\tag{3.14}$$

Further simplifying yields to a quadratic equation for the z-component of the momentum of the neutrino

$$p_z^{\nu 2} - \frac{p_z^\mathrm{l}\delta}{{p_\mathrm{T}^\mathrm{l}}^2}p_z^\nu - \frac{\delta^2}{{p_\mathrm{T}^\mathrm{l}}^2} + \frac{{p_\mathrm{T}^\nu}^2 E^{\mathrm{l}2}}{{p_\mathrm{T}^\mathrm{l}}^2} = 0 \tag{3.15}$$

which has the following solutions

$$p_{z\,1,2}^\nu = \frac{p_z^\mathrm{l}\delta \pm \sqrt{\zeta}}{{p_\mathrm{T}^\mathrm{l}}^2}, \tag{3.16}$$

where

$$\zeta = {p_z^\mathrm{l}}^2\delta^2 - {p_\mathrm{T}^\mathrm{l}}^2 \left[E^{\mathrm{l}2}{p_\mathrm{T}^\nu}^2 - \delta^2\right]. \tag{3.17}$$

There are two possible cases, depending on the sign of ζ. In [5] multiple reconstruction schemes are investigated and the following two are adopted.

Positive ζ

If $\zeta > 0$, both solutions are real and another criterion has to be used to choose one of the two possible solutions. If the product of the two possible solutions $p^{\nu}_{z\,1} \cdot p^{\nu}_{z\,2}$ is negative, the solution with the same sign as the z-component of the lepton p^{l}_z is chosen. Otherwise the solution which results in the smaller partonic center of mass invariant mass is selected.

Negative ζ

In this case, the transverse mass of the lepton neutrino system $M^{\mathrm{l}\nu}_{\mathrm{T}}$ is bigger than the pole Mass M_{W}. For massless particles $m^{\mathrm{l}} = m^{\nu} = 0$, $E_{\mathrm{T}} = p_{\mathrm{T}}$ and therefore the transverse mass can be expressed as:

$$M^{\mathrm{l}\nu}_{\mathrm{T}}{}^2 = m^{\mathrm{l}2} + m^{\nu 2} + 2(E^{\mathrm{l}}_{\mathrm{T}} E^{\nu}_{\mathrm{T}} - \vec{p_{\mathrm{T}}}^{\mathrm{l}} \cdot \vec{p_{\mathrm{T}}}^{\nu}) = 2(p^{\mathrm{l}}_{\mathrm{T}} p^{\nu}_{\mathrm{T}} - \vec{p_{\mathrm{T}}}^{\mathrm{l}} \cdot \vec{p_{\mathrm{T}}}^{\nu}) \tag{3.18}$$

Substituting the transverse mass $M^{\mathrm{l}\nu}_{\mathrm{T}}{}^2$ for the W pole mass M^2_{W} causes $\delta = p^{\mathrm{l}}_{\mathrm{T}} p^{\nu}_{\mathrm{T}}$ and $\zeta = 0$. In this case, the solution for p^{ν}_z reads:

$$p^{\nu}_z = \frac{p^{\mathrm{l}}_z \delta \pm \sqrt{\zeta}}{p^{\mathrm{l}}_{\mathrm{T}}{}^2} = \frac{p^{\mathrm{l}}_z p^{\mathrm{l}}_{\mathrm{T}} p^{\nu}_{\mathrm{T}}}{p^{\mathrm{l}}_{\mathrm{T}}{}^2} = p^{\mathrm{l}}_z \frac{p^{\nu}_{\mathrm{T}}}{p^{\mathrm{l}}_{\mathrm{T}}} \tag{3.19}$$

3.3 Analysis of Monte Carlo Events with Rivet

In this thesis, Rivet-3.1.6 [8] is used to analyze the generated events. Rivet, which stands for "Robust Independent Validation of Experiment and Theory", is a toolkit that can be used for the validation of Monte Carlo event generators. The MC generator Sherpa is equipped with a build-in Rivet support and thus producing input events for a Rivet analysis is very practical.

Every Rivet analysis consists of three analysis event loop methods: `init`, `analyze` and `finalize`. In the `init` method, histograms are booked and projections are initialized before the run. When it comes to per-event aspects of the analysis, these are performed in the `analyze` method. This includes selecting particles and filtering events according to cuts, constructing suitable observables and filling the histograms. Lastly, histograms are normalized and scaled after the run in the `finalize` method.

The complete analysis used in this thesis to analyze the generated events can be found in section A.1. To detect the decaying Z bosons, the `ZFinder` projection is used. Likewise the `WFinder` can be used to find leptonically decaying W bosons, but however, the use of the `WFinder` led to some strange results. Hence an `IdentifiedFinalState` is applied to find the muon, the neutrino is reconstructed from the missing momentum as described in section 3.2. Furthermore Rivet `FastJets` class is utilized to get the momentum of the jets.

4 Study of the Generated Events

In this chapter, the differential distributions for polarized W^+Z scattering in the fully leptonic decay channel are presented for different kinematic observables. Two cases are considered: the W^+ boson has a certain polarization and the Z boson is unpolarized and vice versa. The results are compared with [5], which is from now on referred to as paper.

4.1 Results for a polarized W boson

The polarized and unpolarized total cross sections for a polarized W^+ boson for W^+Z scattering are shown in Table 4.1.
While the difference between the cross section with the full matrix element and the unpolarized one delivers an estimate for so called non resonant effects, the differene between the unpolarized cross section and the polsum provides a rating of the interferences taking place among polarizations. Since lepton cuts are applied, these interferences are not zero. For the paper, the non resonant effects are smaller than 1 % while for Sherpa they are about 1.2 %. We can conclude, that the resonant approximations work quite well in both cases.
As can be seen, the cross sections for the full samples match quite well. The same holds for the longitudinal polarization, but when it comes to the transverse polarization of the W^+ boson, especially the left-handed one, there is a bigger deviation. Hence the values for the

polarization	pol. W^+ [5]	fractions	pol. W^+ Sherpa	fractions Sherpa
full	165.1(1)		165.19(6)	
longitudinal	33.21(3)	0.20698(7)	32.27(4)	0.2070(1)
left handed	96.31(8)	0.6002(1)	93.58(7)	0.60029(1)
right handed	30.93(2)	0.19277(1)	30.03(3)	0.19267(9)
polsum	160.45(9)		155.9(1)	
unpolarized	164.2(2)		163.26(8)	
interferences	3.8(2)		7.34(9)	

Table 4.1: Comparison of polarized and unpolarized total cross sections [ab] for a polarized W^+ boson and an unpolarized Z boson for W^+Z scattering between Sherpa and [5]

polsum also do not match. The same counts for the unpolarized cross section, since the interference effects in Sherpa are roughly twice as big as in the paper. To compensate deviations that can occur due to the fact that the paper uses another approximation than the narrow-width-approximation, the fractions are computed. They are calculated by taking one definite polarization (longitudinal or transverse) and divide it by the polsum. By taking a look at the fractions, we can now see that they agree perfectly. It also stands out, that the W^+ boson is mainly left-handed (60 %) while the longitudinal and right-handed contributions are only about 20.6 % and 19.2 %.

In the following, differential distributions for various observables are shown. The full results are colored in black, the longitudinal ones in red, the left and right polarizations in blue and green and the polsum in violet. In the ratio plot, the ratio of the polsum distribution to the full one is represented. The results for SHERPA are always displayed on the right side, the results from the paper on the left side. In Figure 4.1, the distribution of the invariant mass of the four leptons M_{WZ} for a polarized W^+ boson is shown. The shapes of the histograms coincide rather

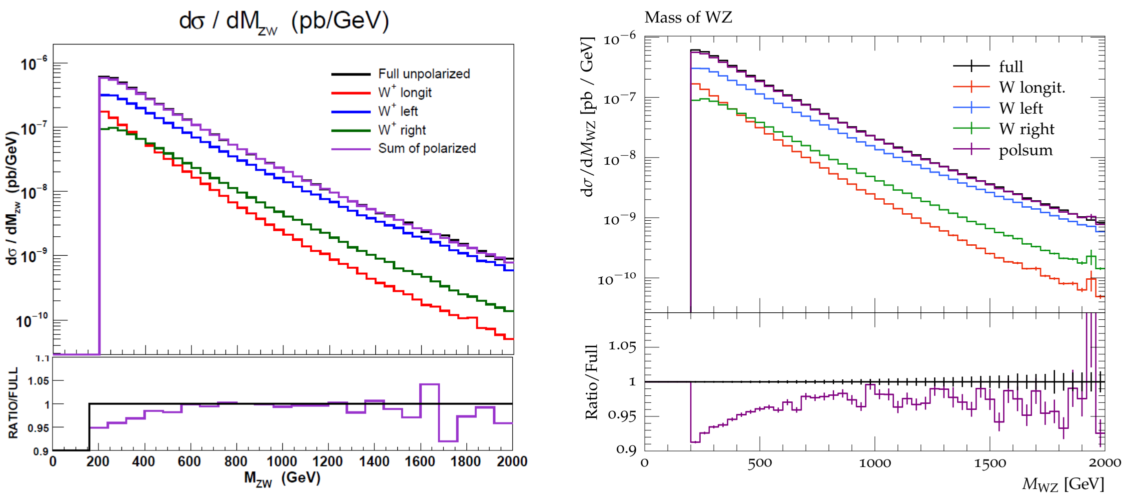

(a) (b)

Figure 4.1: Mass of WZ: Comparison of differential cross sections for a polarized W^+ boson for W^+Z scattering between SHERPA on the right side and [5] on the left

well. As can be seen by the increasing fluctuations, the statistic in the region of large masses is not as good as in the low mass region. This effect is even stronger at the distribution obtained with SHERPA. While the left-handed component remains the largest one over the entire mass range, all fractions, and especially the fraction of the longitudinal polarization, decrease with increasing invariant mass. Figure 4.2 depicts the angular distribution $\cos(\theta_{\mu^+})$ of the muon. If $\cos(\theta_{\mu^+}) = -1$, the muon is radiated in the opposite direction of the boson's flight direction. For $\cos(\theta_{\mu^+}) = 1$ the flight direction of the boson and muon are the same. Given that the weak force violates parity, W^+ bosons only couple to left-handed particles and right-handed anti-particles. For a leptonically decaying W^+ boson follows, that the muon has to be right-handed and the muon neutrino is left-handed (since both particles are considered as massless the helicity is equal to the chirality). Due to the conservation of the spin, if the W^+ boson is now right-handed, the muon has the same flight direction as the boson and therefore $\cos(\theta_{\mu^+}) = 1$. The spin is aligned with the muon's momentum. Whereas the boson is left-handed, the flight direction of the muon and the W^+ boson are contrary to each other, since the muon still has to be right-handed. This correlates with an angle $\cos(\theta_{\mu^+}) = -1$. For longitudinal W^+ bosons,

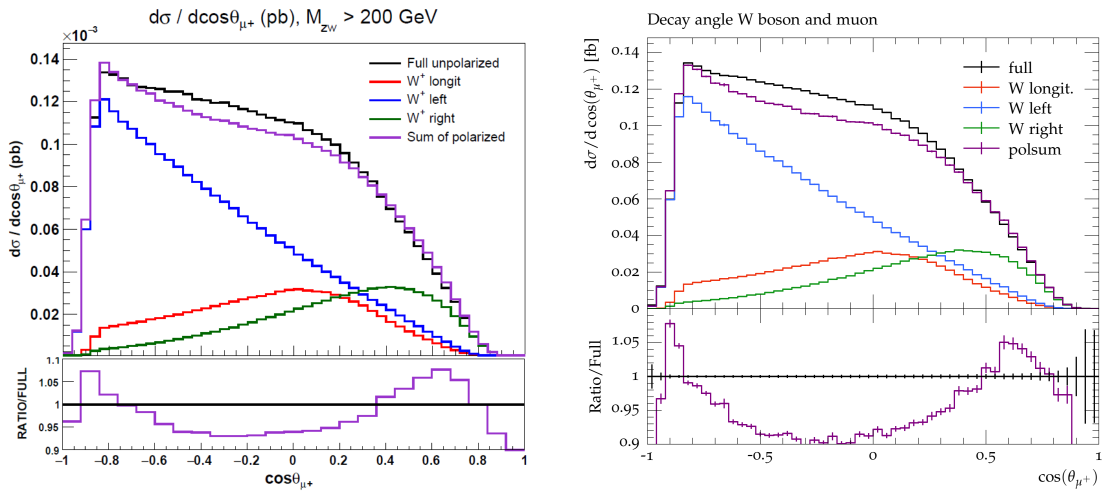

(a) (b)

Figure 4.2: Decay angle W^+ boson and muon: Comparison of differential cross sections for a polarized W^+ boson for W^+Z scattering between SHERPA on the right side and [5] on the left

the expected decay angle is $\frac{\pi}{2}$, which can be associated with $\cos(\theta_{\mu^+}) = 0$. When we look at the distribution for the decay angle of the muon, the longitudinal component actually has its peak at $\cos(\theta_{\mu^+}) = 0$. The blue graph, which correspond to left-handed W^+ bosons, have their maximum at $\cos(\theta_{\mu^+}) \approx -0.8$ which is close to -1. This means that, as described above, the muon is radiated in the opposite direction of the boson's flight direction. Lastly it also stands out, that the peak for right-handed bosons is shifted towards the right edge, which means that the muon travels in the same direction as the boson does.
Especially the applied lepton cuts and the neutrino reconstruction have a big impact on the shape of the distribution, they are responsible for the slightly asymmetric behavior of the longitudinal shape and degrade the peaks of the transverse nodes at the edges of the histogram, where $\theta_{\mu^+} = 0$ or π. When taking a look at the ratio plot, for values between $\cos(\theta_{\mu^+}) \approx -0.8$ and $\cos(\theta_{\mu^+}) \approx 0.6$ the polsum underestimates the full results. In contrast, in the leftover regions, there is also a big discrepancy of a few percent, due to the fact that the interferences become negative. The shape of the histograms in the decay angle plot also approximately follow the normalized distributions in Figure 2.5. But due to the already mentioned transverse momentum cut on the muon and the corresponding neutrino, the shape of the distributions is a little bit blurred for $\cos(\theta_{\mu^+}) \approx -1$ and $\cos(\theta_{\mu^+}) \approx 1$.

The distribution for the pseudorapidity of the W^+ boson can be found in Figure 4.3. The histogram shows a characteristic symmetric shape with a notch right in the middle at $\eta_W = 0$. Responsible for this gap at the central region of the plot is the neutrino reconstruction. Again, when comparing the plot from the paper with the one from SHERPA barely any differences can be seen. Only the greater interference value results in bigger gaps between the full and the polsum sample in the Sherpa plot. The last Figure 4.4 shows the distribution of the transverse

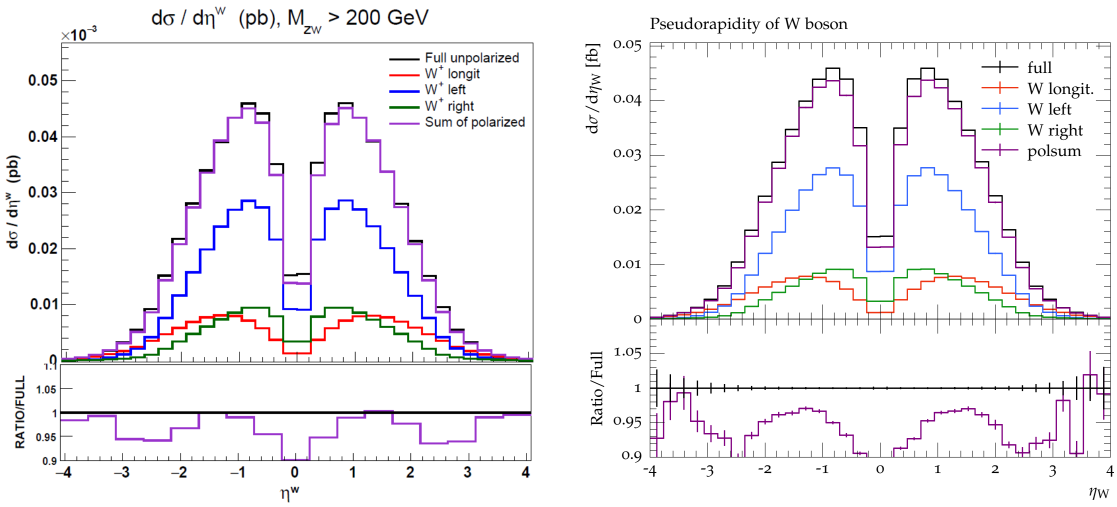

(a) (b)

Figure 4.3: Pseudorapidity of W^+ boson: Comparison of differential cross sections for a polarized W^+ boson for W^+Z scattering between Sherpa on the right side and [5] on the left

momentum of the muon. For increasing transverse momentum, the curves for all polarization settings decrease. For small values of $p_T^{\mu^+}$ the longitudinal and left-handed polarization have a higher cross section. However, with increasing momentum, this behavior flips and for large momenta, W^+ bosons are mainly right-handed and almost no longitudinally polarized bosons are left. As can be seen in the ratio plot, interferences and non resonant effects stay relatively even over the full range of the muon's transverse momentum.

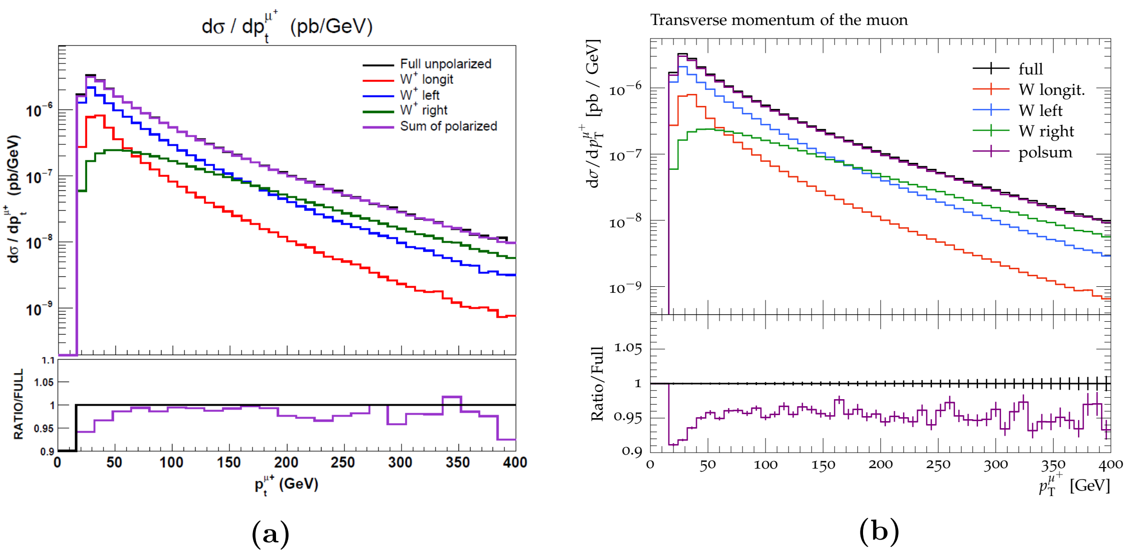

Figure 4.4: Transverse momentum of the muon: Comparison of differential cross sections for a polarized W^+ boson for W^+Z scattering between SHERPA on the right side and [5] on the left

4.2 Results for a polarized Z boson

Now we consider the case in which the Z boson has a particular polarization and therefore the W^+ boson is unpolarized. The polarized and unpolarized total cross sections are shown in Table 4.2. By looking at the longitudinal, left- and right-handed cross sections, it stands out

polarization	pol. Z [5]	fractions	pol. Z SHERPA	fractions SHERPA
full	165.1(1)		165.19(6)	
longitudinal	42.56(3)	0.26604(5)	41.51(4)	0.26628(5)
left handed	76.87(6)	0.4805(1)	74.73(5)	0.47936(4)
right handed	40.54(3)	0.25342(6)	39.65(4)	0.25434(6)
polsum	159.97(8)		155.9(1)	
unpolarized	164.0(2)		163.26(8)	
interferences	4.0(2)		7.34(9)	

Table 4.2: Comparison of polarized and unpolarized total cross sections [ab] for a polarized Z boson and an unpolarized W^+ boson for W^+Z scattering between SHERPA and [5]

that they do not agree with each other. But however, this can be solved when the fractions are taken into account. Again, like in Table 4.1 they match quite well. The Z boson is, like the W^+ boson, mainly left-handed, since this makes up about 48 %. The longitudinal and right-handed components account for only 26.6 % and 25.3 %.

Figure 4.5 depicts the distribution of the invariant mass of the four leptons. Both shapes agree well with each other, and the overall shape is about the same as in Figure 4.1. At masses of about 200 GeV, where the plot starts due to the applied cut, the longitudinal and transverse components of the Z boson are almost equal. But at about 400 GeV they begin to

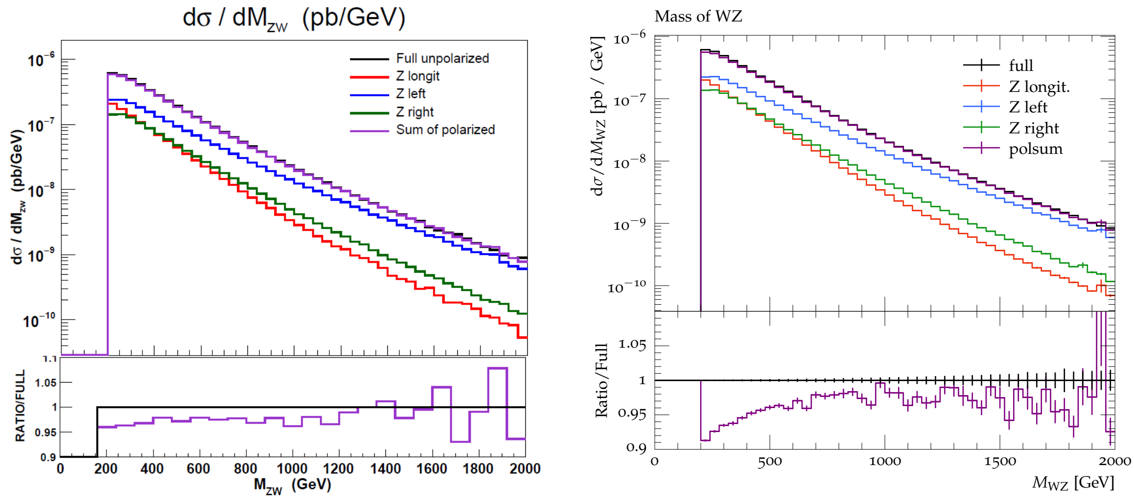

(a) **(b)**

Figure 4.5: Mass of WZ: Comparison of differential cross sections for a polarized Z boson for W^+Z scattering between SHERPA on the right side and [5] on the left

separate from eatch other, as the longitudinal and right-handed polarization decreases faster than the left-handed contributions. At an invariant mass of 2000 GeV almost all Z bosons are left-handed. In Figure 4.6 the distribution for the decay angle of the electron $\cos(\theta_{e^-})$ are

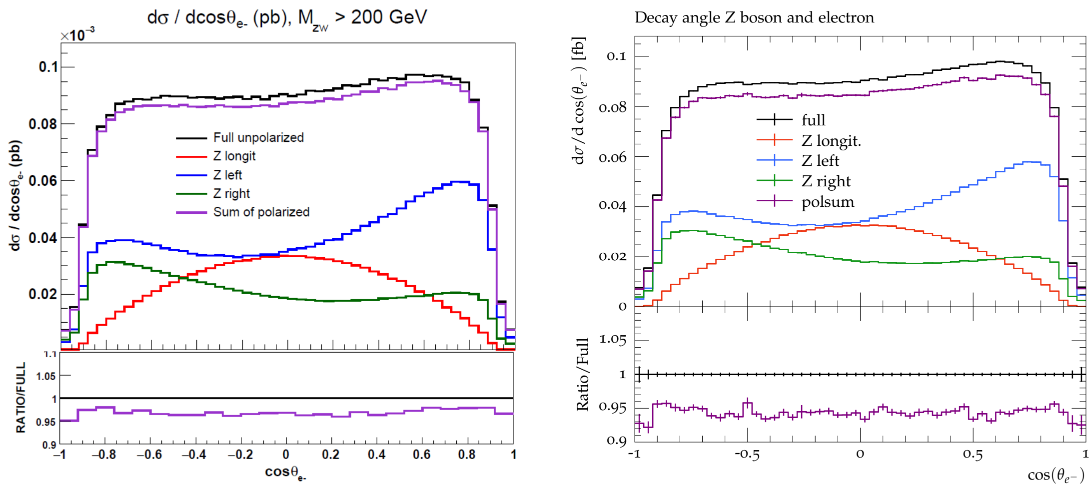

(a) **(b)**

Figure 4.6: Decay angle Z boson and electron: Comparison of differential cross sections for a polarized Z boson for W^+Z scattering between SHERPA on the right side and [5] on the left

shown. The decay angle is the variable, where the most differences for different polarizations can be observed. A distinction between W^+ and Z bosons is their coupling to right-handed particles. Unlike the W^+ boson, the Z boson can couple to right- and left-handed particles with different strength. For longitudinally polarized Z bosons, the peak of the histogram is at $\theta_{e^-} = \frac{\pi}{2}$, which means that the electron is radiated orthogonal to the Z boson's flight direction.

If the electron is radiated along the flight direction of the Z boson, this corresponds to left-handed bosons, since the peak in the plot is shifted to higher values of the decay angle. For electrons that face the opposite direction of the Z boson's momentum, the Z boson can either be left- or right-handed. By comparing the two plots with the distributions in Figure 2.5, one can see that the longitudinal components match quite well and for the transverse components their behavior for big and small decay angle differs a little bit due to some contortions at the edge of the plot. This might be due to the applied transverse momentum cuts for the e^+e^- lepton pair, since they are both charged leptons and therefore for both particles the same cuts were used. In Figure 4.2 the effect is even stronger, since for the muon and for the missing momentum of the neutrino, different transverse momentum cuts are applied.

Figure 4.7 shows the distribution of the pseudorapidity of the Z boson. Compared with

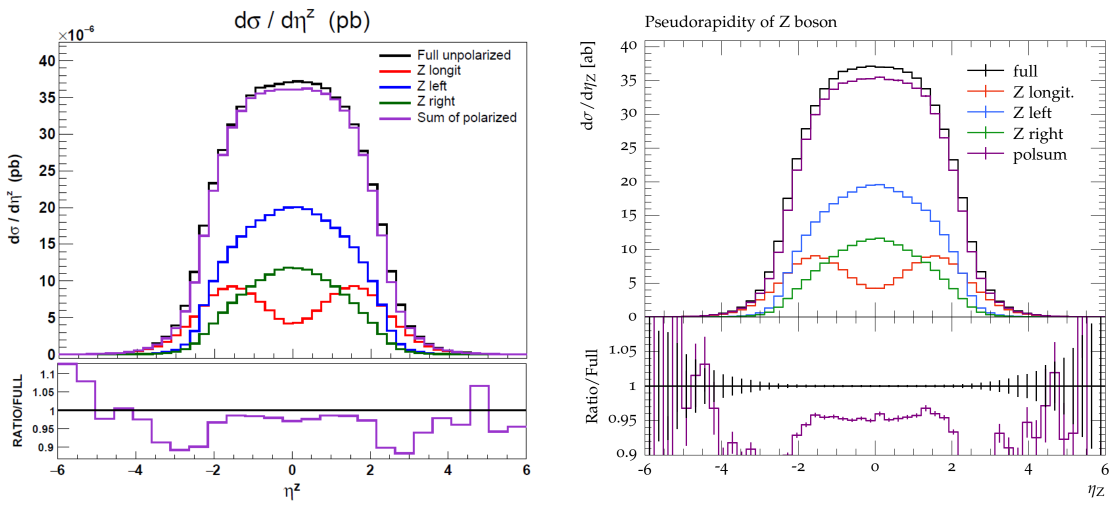

(a) (b)

Figure 4.7: Pseudorapidity of Z boson: Comparison of differential cross sections for a polarized Z boson for W^+Z scattering between SHERPA on the right side and [5] on the left

the distribution of the pseudorapidity of a W^+ boson, we can now see larger interferences of different polarization modes, especially in the regions of $\eta^Z = -2.5$ and $\eta^Z = 2.5$. At $\eta^Z = 0$ the longitudinal component behaves different than the others. While all other components have their maximum at 0, the longitudinal component has a little indentation. Since for all polarizations the distribution drops down towards higher / lower values of the pseudorapidity, the error bars get bigger.

The last contribution we look at is the one for the transverse momentum of the electron in Figure 4.8. The shape is kind of the same as for the transverse momentum of the muon, but now the left-handed polarization dominates for high values of $p_T^{e^-}$. In the lower p_T region the longitudinal and transverse polarizations are roughly of the same order of magnitude and in the higher regions the longitudinal component decreases faster than the transverse polarized contributions. Overall, interferences and non resonant effects are rather small for this plot.

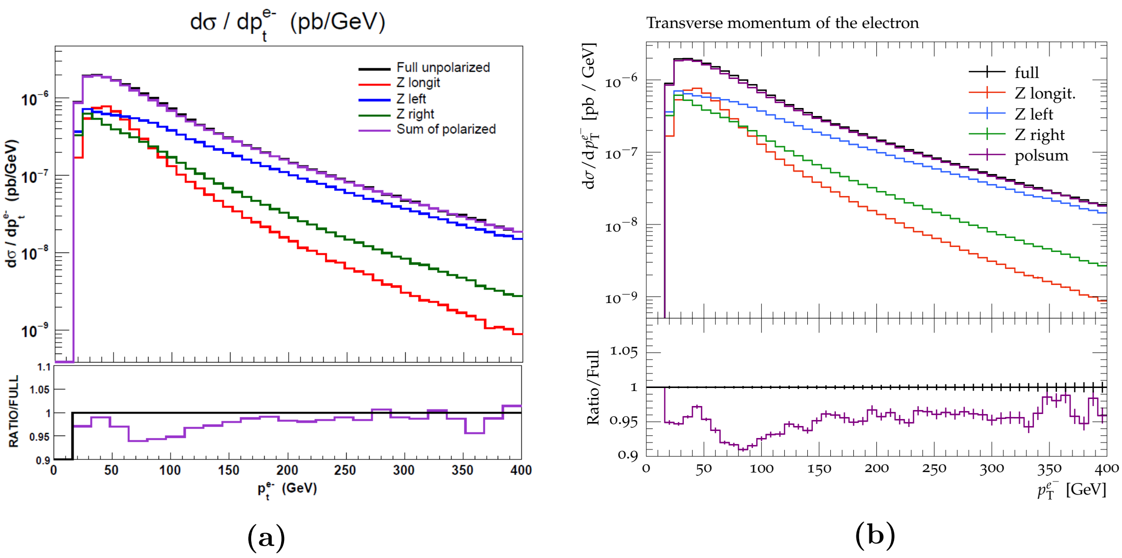

Figure 4.8: Transverse momentum of the electron: Comparison of differential cross sections for a polarized Z boson for W^+Z scattering between SHERPA on the right side and [5] on the left

5 Comparison between Sherpa and MadGraph

In this chapter, the simulated samples are compared with the samples produced in [26].

5.1 Setup of the Simulation

In [26], MADGRAPH-2.9.5 [2] interfaced with PYTHIA8 [7] is used to generate polarized samples for WZ VBS. Thereby PYTHIA is useful for the simulation of shower effects like parton showers and hadronization. Since in [26] the polarization was defined in the rest frame of the W and Z bosons, new samples had to be poduced with SHERPA where the `Referencesystem` definition in the run card was set to `COM`. To get comparable results only the EVNT files for polarized samples denoted with OFP are used. This corresponds to samples, where the leptons associated to the W^+ boson have a different charge than the leptons from the decaying Z bosons. For samples of type OFP, the process definition looks like the following (section B.1.1 in [26]):

```
generate p p > w+{0,T} z{0,T} j j QCD=0, w+ > e+ ve, z > mu+ mu-
add process p p > w+{0,T} z{0,T} j j QCD=0, w+ > mu+ vm, z > e+ e-
```

Given that in section 3.1 only the second process is considered and due to the fact that for the generation of the two processes described above shower effects are active, the RIVET analysis explained in section 3.3 has to be adopted. The altered RIVET analysis can be found in section A.1. To reconstruct the leptons coming from the decaying vector bosons, the `ZFinder` and the `IdentifiedFinalState` projections can no longer be used. Instead one has to use the status codes of the particles. In Monte Carlo Event Generators, every generated particle has a certain decay status. At first, all events that have an incoming or outgoing b quark of the hardest subprocess are rejected. This is achieved by looking at b quarks with a status code of 21 or 23. After that, the extra decay channel where the Z boson decays into muons, has to be filtered out. Therefore all events containing Z bosons with status 62, which have muons as their children, are rejected.

Finally to get the leptons from the hardest subprocess, only W^+ and Z bosons with status code 62, these are outgoing subprocess particles which have the primordial k_{T} included, are taken into account. Then the leptons can be received by calling the children of these bosons. The two quarks, which represent the jets, can be reconstructed by looking at quarks with status code 23. The applied cuts are the same as in section 3.1.

5.2 Study of the Results

In Table 5.1 the polarized total cross sections for polarized W^+ and Z bosons are shown. A "0" behind the W/Z denotes longitudinal polarization, a "T" refers to transverse polarization. By looking at the values we can see that for purely longitudinal and purely transverse polarized bosons, they look quite similar. On the other hand, the mixed components, where one boson is longitudinally polarized and the other one has transverse polarization, differ quite a bit. It is interesting to see, that in both cases for the mixed components, the SHERPA cross section is bigger than the one from the MADGRAPH samples. Even when the fractions are evaluated,

polarization	MADGRAPH	fractions MADGRAPH	SHERPA	fractions SHERPA
W0Z0	12.7(2)	0.0740(8)	12.25(1)	0.06662(4)
W0ZT	24.1(3)	0.140(1)	31.83(5)	0.1731(1)
WTZ0	34.5(3)	0.201(1)	39.24(4)	0.21339(5)
WTZT	100.2(7)	0.584(1)	100.57(9)	0.54687(5)
polsum	171.6(9)		183.9(1)	
unpolarized	173(1)		189.98(9)	
interferences	2.1(3)		6.0(1)	

Table 5.1: Comparison of polarized total cross sections [ab] for different polarization settings for a polarized W^+ and Z boson for W^+Z scattering between MADGRAPH and SHERPA

there is still some discrepancy. However, both predict that the purely transverse polarized contribution accounts for $> 50\,\%$, whereas the purely longitudinal contribution only makes up about $7\,\%$. Like in chapter 4, the interferences in SHERPA are way bigger than the ones in MADGRAPH, here they distinguish by a factor of 3. This could be due to the fact that other approximations than the narrow-width-approximation are used in MADGRAPH.

Figure 5.1 shows two distributions of the decay angle, on the left side for the muon where both vector bosons are longitudinally polarized and on the right hand side for the electron where the W^+ boson is transverse polarized and the Z boson is longitudinally polarized. At first we can see that for both plots the shape of the distributions of SHERPA and MADGRAPH agree with each other. For the decay angle of the muon, this agreement is only suspended for the region where the cosine is zero. By taking a closer look at the distribution for the decay angle of the electron, it stands out that the SHERPA histogram is always above the MADGRAPH one. This can be explained by the higher cross section of the WTZ0 channel for the samples generated with SHERPA. Also, the shape of the differential cross section for the decay angle of the muon looks like the longitudinal W^+ distribution in Figure 4.2. On the other hand, the shape of the differential cross section for the decay angle of the electron looks like the longitudinal Z distribution in Figure 4.6. This makes totally sense, since the W0Z0 channel is part of the channel where the W^+ boson is polarized an the Z boson is unpolarized investigated in section 4.1 and the WTZ0 channel is on his part part of the channel investigated in section 4.2 where a polarized Z boson is investigated. In Figure 5.2

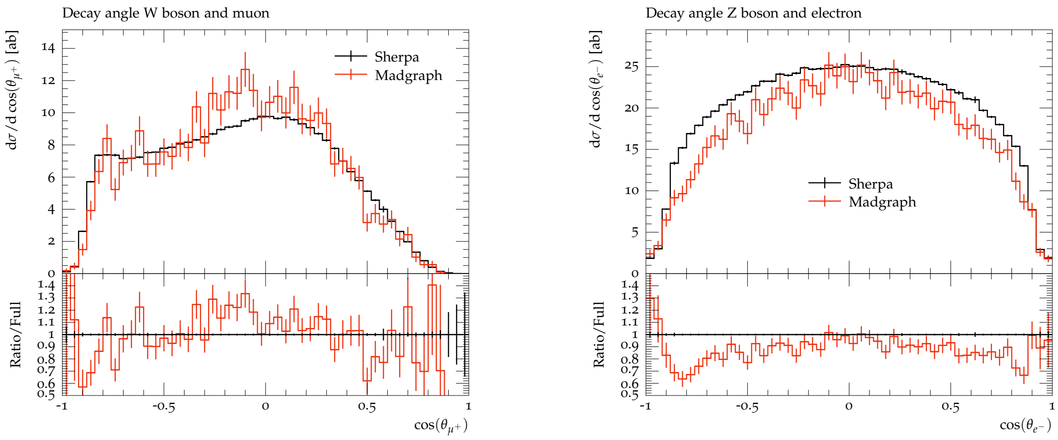

Figure 5.1: Comparison of differential cross sections for the decay angle of the muon for W0Z0 on the left and for the decay angle of the electron for WTZ0 on the right between Sherpa and MadGraph

the differential cross section for the pseudorapidity of the Z boson for W0ZT is shown on the left hand side, while on the right side the distribution for the pseudorapidity of the W^+ boson for WTZT is displayed. By comparing the distributions of Sherpa and MadGraph for the pseudorapidity of the W^+ boson on the right side, we can see that they match perfectly. This

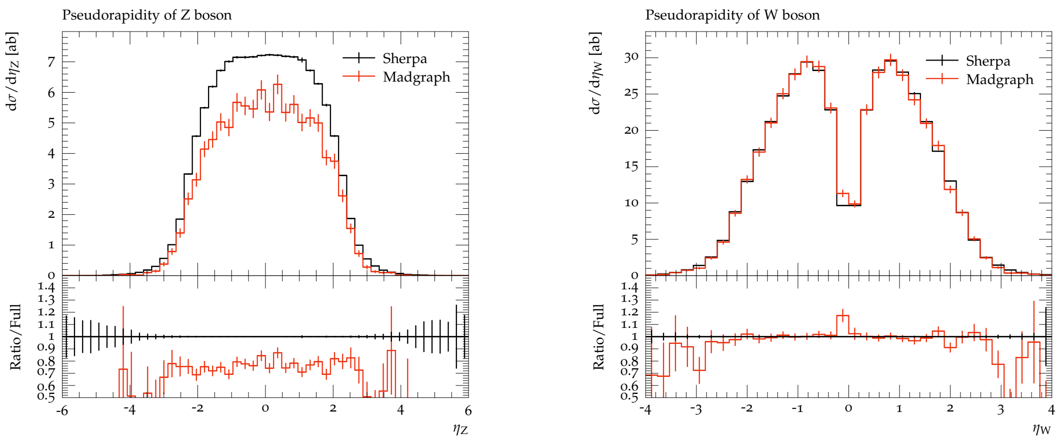

Figure 5.2: Comparison of differential cross sections for the pseudorapidity of the Z boson for W0ZT on the left and for the pseudorapidity of the W^+ boson for WTZT on the right between Sherpa and MadGraph

also corresponds to the matching total cross section of the WTZT channel. However, since that for the W0ZT channel the cross sections do not agree, this also applies for the distributions of the pseudorapidity of the Z boson. Hence, the histogram for Sherpa always lies above the

histogram for MadGraph, but at least the shape is very similar.
Given that the WTZT channel is part of the channel investigated in section 4.1, the distribution of the pseudorapidity of the W^+ boson looks like the ones in Figure 4.3. For a similar reason, the distribution of the pseudorapidity of the Z boson has the same shape as the distributions for left- and right-handed Z bosons in Figure 4.7.

A complete list of all the comparison plots can be found in section A.3. By taking a look at these plots it stands out, that the distributions generated with Sherpa always look smoother, since the histograms produced from the MadGraph samples have quite big error bars. The reason for this is that, as described in section 5.1, all events with initial state b quarks as well as the second channel where the Z boson decays into muons, must be rejected. Hence the number of entries in these histograms is significantly lower.

6 Summary and Outlook

This thesis investigates polarization in the fully leptonic W^+Z channel at the LHC for a center of mass energy of $\sqrt{s} = 13\,\text{TeV}$. The scattering of vector bosons is directly connected to the mechanism of electroweak symmetry breaking, since without a Higgs boson, the scattering of longitudinally polarized gauge bosons violates unitarity. To generate samples with polarization information of the vector bosons, a development version of Sherpa 3.0.0 is used since the current version of Sherpa 2.2.13 can not create such samples.

The received results for the polarized total cross sections as well as for the differential cross sections for different kinematic variables were compared with [5]. To get comparable results, a completely new Rivet analysis was written. When taking a look at the cross sections for the full integration and the polarization fractions, it can be seen that they match quite well. The agreement when looking at the differential cross section distributions was also quite impressing. However it is still unknown why the interference effects are twice as big as in [5]. It can be concluded, that the separation of polarized signals reproduces reliable prognoses for a polarized W^+ and Z boson with applied kinematic cuts and neutrino reconstruction.

In the second part of this thesis, the samples were produced again but this time in the rest frame of the W and Z bosons. The simulated samples were then compared with the samples produced in [26]. Therefore the Rivet analysis was adopted to allow the reconstruction of the particles with the help of Pythia status codes. If both vector bosons (W^+ and Z) are either longitudinally polarized or transverse polarized, the cross sections fit very well. Yet if one of the vector bosons is longitudinally polarized and the other one is transverse polarized, then the cross sections and the fractions distinguish from eatch other. But when looking at the differential cross sections, the shapes match again quite surprsingly. Next steps could involve to either simulate shower effects with Sherpa or to run MadGraph again, this time without shower effects to get a better understanding on how and why the cross sections only differ for polarizations where one boson is transverse polarized and the other one is longitudinally polarized.

In the coming years the LHC will start with the high-luminosity operation at a center of mass energy that is nearly 14 TeV [23]. Hopefully the higher rates that come with the high-luminosity LHC will allow for the observation of longitudinal polarizations. Additionally, new experiments will search for physics beyond the Standard Model.

A Appendix

A.1 Rivet analyses Code

```
// -*- C++ -*-
#include "Rivet/Analysis.hh"
#include "Rivet/Projections/FinalState.hh"
#include "Rivet/Projections/FastJets.hh"
#include "Rivet/Projections/DressedLeptons.hh"
#include "Rivet/Projections/MissingMomentum.hh"
#include "Rivet/Projections/DirectFinalState.hh"
#include "Rivet/Projections/VetoedFinalState.hh"
#include "Rivet/Analyses/MC_JetAnalysis.hh"
#include "Rivet/Projections/ZFinder.hh"
#include "Rivet/Projections/WFinder.hh"
#include "Rivet/Projections/IdentifiedFinalState.hh"
#include "Rivet/Projections/PromptFinalState.hh"
#include "Rivet/Particle.hh"


namespace Rivet {

  /// @brief W^+[munu]Z[ee] + jets
  class MC_WZjj_LAB : public Analysis {
  public:

    /// Default Constructor
    MC_WZjj_LAB()
      : Analysis("MC_WZjj_LAB")
    {     }

    /// @name Analysis methods
    /// @{

    // Transformation of the lepton into W boson rest frame
    Vector3 BoostAndRotate_LabFr(const FourMomentum m_boost, const FourMomentum m_momentum) {
            const LorentzTransform m_transform = LorentzTransform::mkObjTransformFromBeta(-(
                m_boost.betaVec()));
            Matrix3 l_zrot(m_boost.vector3(), Vector3(0.0, 0.0, 1.0));
            return l_zrot*(m_transform.transform(m_momentum).vector3());
    }

    /// Book histograms and initialise projections before the run
    void init() {
      // ZFinder: Z boson decay into electron + positron with cuts
      FinalState fs;
      ZFinder zeefinder(fs, Cuts::abseta < 2.5 && Cuts::pT > 20*GeV, PID::ELECTRON, 76.1876*
          GeV, 106.1876*GeV, 0.2);
      declare(zeefinder, "ZeeFinder");
```

```

      // Muon final state with cuts
      IdentifiedFinalState ifsLeptons(Cuts::abseta < 2.5 && Cuts::pT > 20*GeV);
      ifsLeptons.acceptIdPair(PID::MUON);
      declare(ifsLeptons, "projLeptons");

      // Missing momentum
      declare(MissingMomentum(fs), "MET");

      // Jets final state
      VetoedFinalState jetinput;
      jetinput
          .addVetoOnThisFinalState(zeefinder)
          .addVetoOnThisFinalState(ifsLeptons);
      FastJets jetpro(jetinput, FastJets::ANTIKT, 0.4);
      declare(jetpro, "Jets");

      // Book histograms
      book(_h_WZ_m ,"WZ_m", 50, 0, 2000);
      book(_h_W_eta ,"W_eta", 34, -4.0, 4.0);
      book(_h_Z_eta ,"Z_eta", 50, -6.0, 6.0);
      book(_h_W_costheta ,"W_costheta", 50, -1.0, 1.0);
      book(_h_Mu_pT, "Mu_pT", 50, 0, 400);
      book(_h_Z_costheta,"Z_costheta", 50, -1.0, 1.0);
      book(_h_Em_pT, "Em_pT", 50, 0, 400);
      book(_h_WZ_WQ, "WZ_WQ", 1, 0.0, 1.0);
    }


    /// Perform the per-event analysis
    void analyze(const Event& e) {
      // Apply ZFinder
      const ZFinder& zeefinder = apply<ZFinder>(e, "ZeeFinder");
      if (zeefinder.bosons().size() !=1) vetoEvent;

      // Z boson, electron, positron momentum
      const FourMomentum& zee = zeefinder.bosons()[0].momentum();
      const FourMomentum& ep = zeefinder.constituents()[0].momentum();
      const FourMomentum& em = zeefinder.constituents()[1].momentum();

      // Muon momentum
      const Particles& ifsLeptons = apply<IdentifiedFinalState>(e, "projLeptons").
          particlesByPt();
      if (ifsLeptons.size() !=1) vetoEvent;
      const FourMomentum& mp = ifsLeptons[0].momentum();

      // Jet momentum with cuts
      const Jets& jets = apply<FastJets>(e, "Jets").jetsByPt(Cuts::pT > 20*GeV && Cuts::
          abseta < 5.0);
      if (jets.size() != 2) vetoEvent;
      const FourMomentum j0 = jets[0].momentum();
      const FourMomentum j1 = jets[1].momentum();

      // Jet cuts
      const FourMomentum j01 = j0 + j1;
      double mj01 = j01.mass();
      double AbsdEtajj = fabs(j0.eta() - j1.eta());
      if ((mj01 <= 500*GeV) || (AbsdEtajj <= 2.5)) vetoEvent;
```

```

    // Apply a missing-momentum cut
    if (apply<MissingMomentum>(e, "MET").missingPt() <= 40*GeV)  vetoEvent;

    // Neutrino reconstruction
    const ThreeMomentum& missingmomentum = apply<MissingMomentum>(e, "MET").vectorPtMiss();
    double mnu_px = missingmomentum.px();
    double mnu_py = missingmomentum.py();
    double mnu_pz;

    const double M_W = 80.358;
    double xi = M_W * M_W / 2 + mp.pTvec().dot(missingmomentum.pTvec());
    double Delta = mp.pz() * mp.pz() * xi * xi - mp.pT() * mp.pT() * (mp.E() * mp.E() *
        missingmomentum.pT() * missingmomentum.pT() - xi * xi);

    double mnu_pz1 = (mp.pz() * xi + sqrt(Delta)) / (mp.pT() * mp.pT());
    double mnu_pz2 = (mp.pz() * xi - sqrt(Delta)) / (mp.pT() * mp.pT());

    if (Delta > 0)
    {
        if (mnu_pz1 * mnu_pz2 < 0)
        {
            if (mnu_pz1 * mp.pz() > 0)
            {
              mnu_pz = mnu_pz1;
            }
            else
            {
              mnu_pz = mnu_pz2;
            }
        }
        else
        {
          double E1 = sqrt(mnu_px * mnu_px + mnu_py * mnu_py + mnu_pz1 * mnu_pz1);
          double E2 = sqrt(mnu_px * mnu_px + mnu_py * mnu_py + mnu_pz2 * mnu_pz2);
          const FourMomentum mnu1 = FourMomentum(E1, mnu_px, mnu_py, mnu_pz1);
          const FourMomentum mnu2 = FourMomentum(E2, mnu_px, mnu_py, mnu_pz2);
          const FourMomentum P1 = mp + ep + em + mnu1 + j0 + j1;
          double M1 = P1.mass();
          const FourMomentum P2 = mp + ep + em + mnu2 + j0 + j1;
          double M2 = P2.mass();

          if (M1 < M2)
          {
            mnu_pz = mnu_pz1;
          }
          else
          {
            mnu_pz = mnu_pz2;
          }
        }
    }
    else
    {
        mnu_pz = mp.pz() * missingmomentum.pT() / mp.pT();
    }

    // Construct neutrino momentum
```

```
      double E = sqrt(mnu_px * mnu_px + mnu_py * mnu_py + mnu_pz * mnu_pz);
      const FourMomentum mnu = FourMomentum(E, mnu_px, mnu_py, mnu_pz);

      // W boson momentum
      const FourMomentum wmnu = mp + mnu;

      // WZ momentum
      const FourMomentum wz = zee + wmnu;

      // Cut mass WZ
      double mwz = wz.mass();
      if (mwz <= 200*GeV) vetoEvent;

      // Fill histograms
      double mwz2=wz.mass2();
      if (mwz2>0.0) _h_WZ_m->fill(sqrt(mwz2)/GeV);

      _h_W_eta->fill(wmnu.eta());
      _h_Z_eta->fill(zee.eta());
      _h_Mu_pT->fill(mp.pT()/GeV);
      _h_Em_pT->fill(em.pT()/GeV);

      // Muon momentum transformation into W boson rest frame
      Vector3 mp_rotiert = BoostAndRotate_LabFr(wmnu, mp);

      // Compute decay angle muon
      const Vector3 v_z = Vector3(0.0, 0.0, 1.0);
      double cos_theta_mp = mp_rotiert.dot(v_z) / (mp_rotiert.mod() * v_z.mod());
      _h_W_costheta->fill(cos_theta_mp);

      // Electron momentum transformation into Z boson rest frame
      Vector3 em_rotiert = BoostAndRotate_LabFr(zee, em);

      // Compute decay angle electron
      double cos_theta_em = em_rotiert.dot(v_z) / (em_rotiert.mod() * v_z.mod());
      _h_Z_costheta->fill(cos_theta_em);

      // Cross-section
      _h_WZ_WQ->fill(0.5);
    }


    /// Finalize: Normalise histograms etc., after the run
    void finalize() {
      const double s = crossSection()/picobarn/sumOfWeights();

      scale(_h_WZ_m, s);
      scale(_h_W_eta, s);
      scale(_h_Z_eta, s);
      scale(_h_W_costheta, s);
      scale(_h_Mu_pT, s);
      scale(_h_Z_costheta, s);
      scale(_h_Em_pT, s);
      scale(_h_WZ_WQ, s);
    }

    /// @}

```

```
private:

    /// @name Histograms
    /// @{
    Histo1DPtr _h_WZ_m;
    Histo1DPtr _h_W_eta;
    Histo1DPtr _h_Z_eta;
    Histo1DPtr _h_W_costheta;
    Histo1DPtr _h_Mu_pT;
    Histo1DPtr _h_Z_costheta;
    Histo1DPtr _h_Em_pT;
    Histo1DPtr _h_WZ_WQ;
    /// @}
  };

// The hook for the plugin system
  RIVET_DECLARE_PLUGIN(MC_WZjj_LAB);

}
```

Listing A.1: Rivet analysis for $W^+ (\mu^+\nu_\mu)\ Z\,(e^+e^-)$ + jets production

```
// -*- C++ -*-
#include "Rivet/Analysis.hh"
#include "Rivet/Projections/FinalState.hh"
#include "Rivet/Projections/FastJets.hh"
#include "Rivet/Projections/DressedLeptons.hh"
#include "Rivet/Projections/MissingMomentum.hh"
#include "Rivet/Projections/DirectFinalState.hh"
#include "Rivet/Projections/VetoedFinalState.hh"
#include "Rivet/Analyses/MC_JetAnalysis.hh"
#include "Rivet/Projections/ZFinder.hh"
#include "Rivet/Projections/WFinder.hh"
#include "Rivet/Projections/IdentifiedFinalState.hh"
#include "Rivet/Projections/PromptFinalState.hh"
#include "Rivet/Particle.hh"


namespace Rivet {

  /// @brief W^+[munu]Z[ee] + jets
  class MC_WZjj_Madgraph : public Analysis {
  public:

    /// Default Constructor
    MC_WZjj_Madgraph()
      : Analysis("MC_WZjj_Madgraph")
    {    }

    /// @name Analysis methods
    /// @{

    // Transformation of the lepton into W boson rest frame
    Vector3 BoostAndRotate_LabFr(const FourMomentum m_boost, const FourMomentum m_momentum) {
            const LorentzTransform m_transform = LorentzTransform::mkObjTransformFromBeta(-(
                m_boost.betaVec()));
            Matrix3 l_zrot(m_boost.vector3(), Vector3(0.0, 0.0, 1.0));
            return l_zrot*(m_transform.transform(m_momentum).vector3());
```

```
    }

    /// Book histograms and initialise projections before the run
    void init() {
      // Counter for number of events and vetos
      counter0 = 0;
      counter1 = 0;
      counterVeto = 0;

      // Book histograms
      book(_h_WZ_m ,"WZ_m", 50, 0, 2000);
      book(_h_W_eta ,"W_eta", 34, -4.0, 4.0);
      book(_h_Z_eta ,"Z_eta", 50, -6.0, 6.0);
      book(_h_W_costheta ,"W_costheta", 50, -1.0, 1.0);
      book(_h_Mu_pT, "Mu_pT", 50, 0, 400);
      book(_h_Z_costheta,"Z_costheta", 50, -1.0, 1.0);
      book(_h_Em_pT, "Em_pT", 50, 0, 400);
      book(_h_WZ_WQ, "WZ_WQ", 1, 0.0, 1.0);
    }


    /// Perform the per-event analysis
    void analyze(const Event& e) {
      counter0++;

      // Define particle momentum
      FourMomentum j0;
      FourMomentum j1;
      FourMomentum ep;
      FourMomentum em;
      FourMomentum mp;
      ThreeMomentum missingmomentum;

      std::vector<Particle> teilchen_ZBosonen;
      std::vector<Particle> teilchen_WBosonen;
      std::vector<Particle> teilchen_quarks;
      std::vector<Particle> elektron;
      std::vector<Particle> positron;
      std::vector<Particle> antimyon;
      std::vector<Particle> myonneutrino;
      double mnu_px;
      double mnu_py;

      // Get access to all particles in the event
      int i;
      const Particles teilchen = e.allParticles();
      int l = teilchen.size();

      // Veto conditions
      for (i=0; i < l; i++) {
        // Veto b quarks
        if (teilchen[i].genParticle()->status() == 21 && teilchen[i].abspid() == 5)
            counterVeto++;
        if (teilchen[i].genParticle()->status() == 21 && teilchen[i].abspid() == 5) vetoEvent
            ;
        if (teilchen[i].genParticle()->status() == 23 && teilchen[i].abspid() == 5)
            counterVeto++;
        if (teilchen[i].genParticle()->status() == 23 && teilchen[i].abspid() == 5) vetoEvent
```

```
        ;

    // Veto decay channel Z -> Muon
    if ((teilchen[i].pid() == 23) && (teilchen[i].genParticle()->status() == 62) && (
        teilchen[i].children()[0].abspid() == 13)) counterVeto++;
    if ((teilchen[i].pid() == 23) && (teilchen[i].genParticle()->status() == 62) && (
        teilchen[i].children()[0].abspid() ==13)) vetoEvent;
  }

  int u;
  // Find bosons, leptons and quarks
  for (u=0; u < l; u++) {
    // Z boson as an outgoing subprocess particle (primordial kT included) + leptons
    if (teilchen[u].pid() == 23 && teilchen[u].genParticle()->status()==62) {
      teilchen_ZBosonen.push_back(teilchen[u]);
      positron.push_back(teilchen[u].children()[0]);
      elektron.push_back(teilchen[u].children()[1]);
    }

    // W boson as an outgoing subprocess particle (primordial kT included) + leptons
    if (teilchen[u].pid() == 24 && teilchen[u].genParticle()->status()==62) {
      teilchen_WBosonen.push_back(teilchen[u]);
      antimyon.push_back(teilchen[u].children()[0]);
      myonneutrino.push_back(teilchen[u].children()[1]);
    }

    // Quarks
    if (teilchen[u].genParticle()->status() == 23) {
      if ((teilchen[u].abspid() == 1) || (teilchen[u].abspid() == 2) || (teilchen[u].
          abspid() == 3) || (teilchen[u].abspid() == 4)) {
        teilchen_quarks.push_back(teilchen[u]);
      }
    }
  }

  // Veto if no W/Z boson were found
  if (teilchen_ZBosonen.size() == 0) vetoEvent;
  if (teilchen_WBosonen.size() == 0) vetoEvent;

  // Allocate particle momentum
  em = elektron[0].momentum();
  ep = positron[0].momentum();
  mp = antimyon[0].momentum();
  mnu_px = myonneutrino[0].momentum().px();
  mnu_py = myonneutrino[0].momentum().py();

  // Jets by pT
  int j0pt = teilchen_quarks[0].momentum().pT();
  int j1pt = teilchen_quarks[1].momentum().pT();
  if (j0pt > j1pt) {
    j0 = teilchen_quarks[0].momentum();
    j1 = teilchen_quarks[1].momentum();
  }
  else {
    j0 = teilchen_quarks[1].momentum();
    j1 = teilchen_quarks[0].momentum();
  }

```

```
      // Construct 3-momentum of neutrino
      missingmomentum = ThreeMomentum(mnu_px, mnu_py, 0.0);

      // Z boson momentum
      const FourMomentum& zee = ep + em;
      const double mz = zee.mass();

      // Lepton cuts
      if (fabs(mz - 91.153) >= 15*GeV) vetoEvent;
      if (ep.abseta() >= 2.5) vetoEvent;
      if (em.abseta() >= 2.5) vetoEvent;
      if (mp.abseta() >= 2.5) vetoEvent;
      if (ep.pT() <= 20*GeV) vetoEvent;
      if (em.pT() <= 20*GeV) vetoEvent;
      if (mp.pT() <= 20*GeV) vetoEvent;
      if (missingmomentum.pT() <= 40*GeV) vetoEvent;

      // Jet cuts
      if (j0.pT() <= 20*GeV) vetoEvent;
      if (j0.abseta() >= 5.0) vetoEvent;
      if (j1.pT() <= 20*GeV) vetoEvent;
      if (j1.abseta() >= 5.0) vetoEvent;

      const FourMomentum j01 = j0 + j1;
      double mj01 = j01.mass();
      double AbsdEtajj = fabs(j0.eta() - j1.eta());
      if ((mj01 <= 500*GeV) || (AbsdEtajj <= 2.5)) vetoEvent;

      // Neutrino reconstruction
      double mnu_pz;
      const double M_W = 80.358;
      double xi = M_W * M_W / 2 + mp.pTvec().dot(missingmomentum.pTvec());
      double Delta = mp.pz() * mp.pz() * xi * xi - mp.pT() * mp.pT() * (mp.E() * mp.E() *
          missingmomentum.pT() * missingmomentum.pT() - xi * xi);

      double mnu_pz1 = (mp.pz() * xi + sqrt(Delta)) / (mp.pT() * mp.pT());
      double mnu_pz2 = (mp.pz() * xi - sqrt(Delta)) / (mp.pT() * mp.pT());

      if (Delta > 0)
      {
          if (mnu_pz1 * mnu_pz2 < 0)
          {
              if (mnu_pz1 * mp.pz() > 0)
              {
                mnu_pz = mnu_pz1;
              }
              else
              {
                mnu_pz = mnu_pz2;
              }
          }
          else
          {
            double E1 = sqrt(mnu_px * mnu_px + mnu_py * mnu_py + mnu_pz1 * mnu_pz1);
            double E2 = sqrt(mnu_px * mnu_px + mnu_py * mnu_py + mnu_pz2 * mnu_pz2);
            const FourMomentum mnu1 = FourMomentum(E1, mnu_px, mnu_py, mnu_pz1);
            const FourMomentum mnu2 = FourMomentum(E2, mnu_px, mnu_py, mnu_pz2);
            const FourMomentum P1 = mp + ep + em + mnu1 + j0 + j1;
```

```
              double M1 = P1.mass();
              const FourMomentum P2 = mp + ep + em + mnu2 + j0 + j1;
              double M2 = P2.mass();

              if (M1 < M2)
              {
                mnu_pz = mnu_pz1;
              }
              else
              {
                mnu_pz = mnu_pz2;
              }
            }
        }
        else
        {
            mnu_pz = mp.pz() * missingmomentum.pT() / mp.pT();
        }

        // Construct neutrino momentum
        double E = sqrt(mnu_px * mnu_px + mnu_py * mnu_py + mnu_pz * mnu_pz);
        const FourMomentum mnu = FourMomentum(E, mnu_px, mnu_py, mnu_pz);

        // W boson momentum
        const FourMomentum wmnu = mp + mnu;

        // WZ momentum
        const FourMomentum wz = zee + wmnu;

        // Cut mass WZ
        double mwz = wz.mass();
        if (mwz <= 200*GeV) vetoEvent;

        // Fill histograms
        double mwz2=wz.mass2();
        if (mwz2>0.0) _h_WZ_m->fill(sqrt(mwz2)/GeV);

        _h_W_eta->fill(wmnu.eta());
        _h_Z_eta->fill(zee.eta());
        _h_Mu_pT->fill(mp.pT()/GeV);
        _h_Em_pT->fill(em.pT()/GeV);

        // Muon momentum transformation into W boson rest frame
        Vector3 mp_rotiert = BoostAndRotate_LabFr(wmnu, mp);

        // Compute decay angle muon
        const Vector3 v_z = Vector3(0.0, 0.0, 1.0);
        double cos_theta_mp = mp_rotiert.dot(v_z) / (mp_rotiert.mod() * v_z.mod());
        _h_W_costheta->fill(cos_theta_mp);

        // Electron momentum transformation into Z boson rest frame
        Vector3 em_rotiert = BoostAndRotate_LabFr(zee, em);

        // Compute decay angle electron
        double cos_theta_em = em_rotiert.dot(v_z) / (em_rotiert.mod() * v_z.mod());
        _h_Z_costheta->fill(cos_theta_em);

        // Cross-section
```

```
      _h_WZ_WQ->fill(0.5);

      counter1++;
    }

    /// Finalize: Normalise histograms etc., after the run
    void finalize() {
      const double s = crossSection()/picobarn/sumOfWeights();

      scale(_h_WZ_m, s);
      scale(_h_W_eta, s);
      scale(_h_Z_eta, s);
      scale(_h_W_costheta, s);
      scale(_h_Mu_pT, s);
      scale(_h_Z_costheta, s);
      scale(_h_Em_pT, s);
      scale(_h_WZ_WQ, s);
    }

    /// @}

private:

    /// @name Histograms
    /// @{
    Histo1DPtr _h_WZ_m;
    Histo1DPtr _h_W_eta;
    Histo1DPtr _h_Z_eta;
    Histo1DPtr _h_W_costheta;
    Histo1DPtr _h_Mu_pT;
    Histo1DPtr _h_Z_costheta;
    Histo1DPtr _h_Em_pT;
    Histo1DPtr _h_WZ_WQ;

    int counter0;
    int counter1;
    int counterVeto;
    /// @}
  };

// The hook for the plugin system
  RIVET_DECLARE_PLUGIN(MC_WZjj_Madgraph);

}
```

Listing A.2: Rivet analysis for $W^+(\mu^+\nu_\mu)\, Z(e^+e^-)$ + jets production using Pythia status codes

A.2 Sherpa data cards

```
# Sherpa configuration for W^{+}Z+Jets production and decay into leptons

# set up beams for LHC run 2
BEAMS: 2212
BEAM_ENERGIES: 6500
```

```

# Switch off multiparton interactions
MI_HANDLER: None    # Amisic

# Switch off Shower generator
SHOWER_GENERATOR: None

# no hadronisation
FRAGMENTATION: None

# switch off QED corrections
ME_QED: {ENABLED: false}

# matrix-element calculation
ME_GENERATORS:
- Comix

# BEAM_REMNANTS do not work without showers
BEAM_REMNANTS: false

# parton density function
PDF_LIBRARY: LHAPDFSherpa
PDF_SET: NNPDF30_lo_as_0130
ALPHAS: {USE_PDF: 1}

EW_scheme: Gmu
GF: 0.0000116637
GMU_CMS_AQED_CONVENTION: 4

EVENT_GENERATION_MODE: Weighted

# factorization scale mu = M_4l / sqrt(2)
SCALES: VAR{Abs2(p[2]+p[3]+p[4]+p[5])/2}

# number of events
EVENTS: 500000

# exclude bottom quark
PARTICLE_DATA:
  5:
    Active: false
  24:
    Mass: 80.358
    Width: 2.084
  23:
    Mass: 91.153
    Width: 2.494

YFS:
  MODE: None

PSI:
  ITMIN_BY_NODE: 2000

COMIX:
  VSOPT: 5

INTEGRATION_ERROR: 0.05
```

```

HARD_DECAYS:
  QED_Corrections: 0

# pp -> W^{+}Zjj -> e+ e- mu+ nu_mu j j
PROCESSES:
- 93 93 -> 11 -11 -13 14 93 93:
    Order: {QCD: 0, EW: 6}

# Cuts
SELECTORS:
- [Mass, 11, -11, 76.153, 106.153]

- FastjetSelector:
    Expression: Mass(p[6]+p[7])>500
    Algorithm: antikt
    N: 2
    PTMin: 20
    EtaMax: 5

- FastjetSelector:
    Expression: abs(DEta(p[6], p[7]))>2.5
    Algorithm: antikt
    N: 2
    PTMin: 20
    EtaMax: 5

- [Eta, 11, -2.5, 2.5]

- [Eta, -11, -2.5, 2.5]

- [Eta, -13, -2.5, 2.5]

- [PT, 11, 20, E_CMS]

- [PT, -11, 20, E_CMS]

- [PT, -13, 20, E_CMS]

- [PTmis, 40, E_CMS]

# analysis
ANALYSIS: Rivet
RIVET:
  --analyses:
    - MC_WZjj_LAB
  --ignore-beams: 1
```

Listing A.3: Sherpa file for full sample

```
# Sherpa configuration for W^{+}Z+Jets production and decay into leptons

# set up beams for LHC run 2
BEAMS: 2212
BEAM_ENERGIES: 6500

# Switch off multiparton interactions
MI_HANDLER: None   # Amisic
```

```

# Switch off Shower generator
SHOWER_GENERATOR: None

# no hadronisation
FRAGMENTATION: None

# switch off QED corrections
ME_QED: {ENABLED: false}

# matrix-element calculation
ME_GENERATORS:
- Comix

# BEAM_REMNANTS do not work without showers
BEAM_REMNANTS: false

# parton density function
PDF_LIBRARY: LHAPDFSherpa
PDF_SET: NNPDF30_lo_as_0130
ALPHAS: {USE_PDF: 1}

EW_scheme: Gmu
GF: 0.0000116637
GMU_CMS_AQED_CONVENTION: 4

EVENT_GENERATION_MODE: Weighted

# factorization scale mu = M_4l / sqrt(2)
SCALES: VAR{Abs2(p[2]+p[3])/2}

# number of events
EVENTS: 500000

# exclude bottom quark
PARTICLE_DATA:
  5:
    Active: false
  24:
    Mass: 80.358
    Width: 0
  23:
    Mass: 91.153
    Width: 0

YFS:
   MODE: None

PSI:
   ITMIN_BY_NODE: 2000

COMIX:
   VSOPT: 5

INTEGRATION_ERROR: 0.05

# boson decay
HARD_DECAYS:
```

```
  Enabled: true
  Mass_Smearing: 1
  Channels:
    23, 11, -11: { Status: 2 }
    24, -13, 14: { Status: 2 }
  QED_Corrections: 0

# pp -> W^{+}Zjj
PROCESSES:
- 93 93 -> 23 24 93 93:
    Order: {QCD: 0, EW: 4}

# polarization
POL_CROSS_SECTION:
  Enabled: true
  Weight1: 2
  Weight2: 3
q
# Cuts
SELECTORS:
- FastjetSelector:
    Expression: Mass(p[4]+p[5])>500
    Algorithm: antikt
    N: 2
    PTMin: 20
    EtaMax: 5

- FastjetSelector:
    Expression: abs(DEta(p[4], p[5]))>2.5
    Algorithm: antikt
    N: 2
    PTMin: 20
    EtaMax: 5

# analysis
ANALYSIS: Rivet
RIVET:
  --analyses:
    - MC_WZjj_LAB
  --ignore-beams: 1
```

Listing A.4: Sherpa file including polarization settings for W^+ and Z bosons

A.3 Comparison Plots for Sherpa and MadGraph

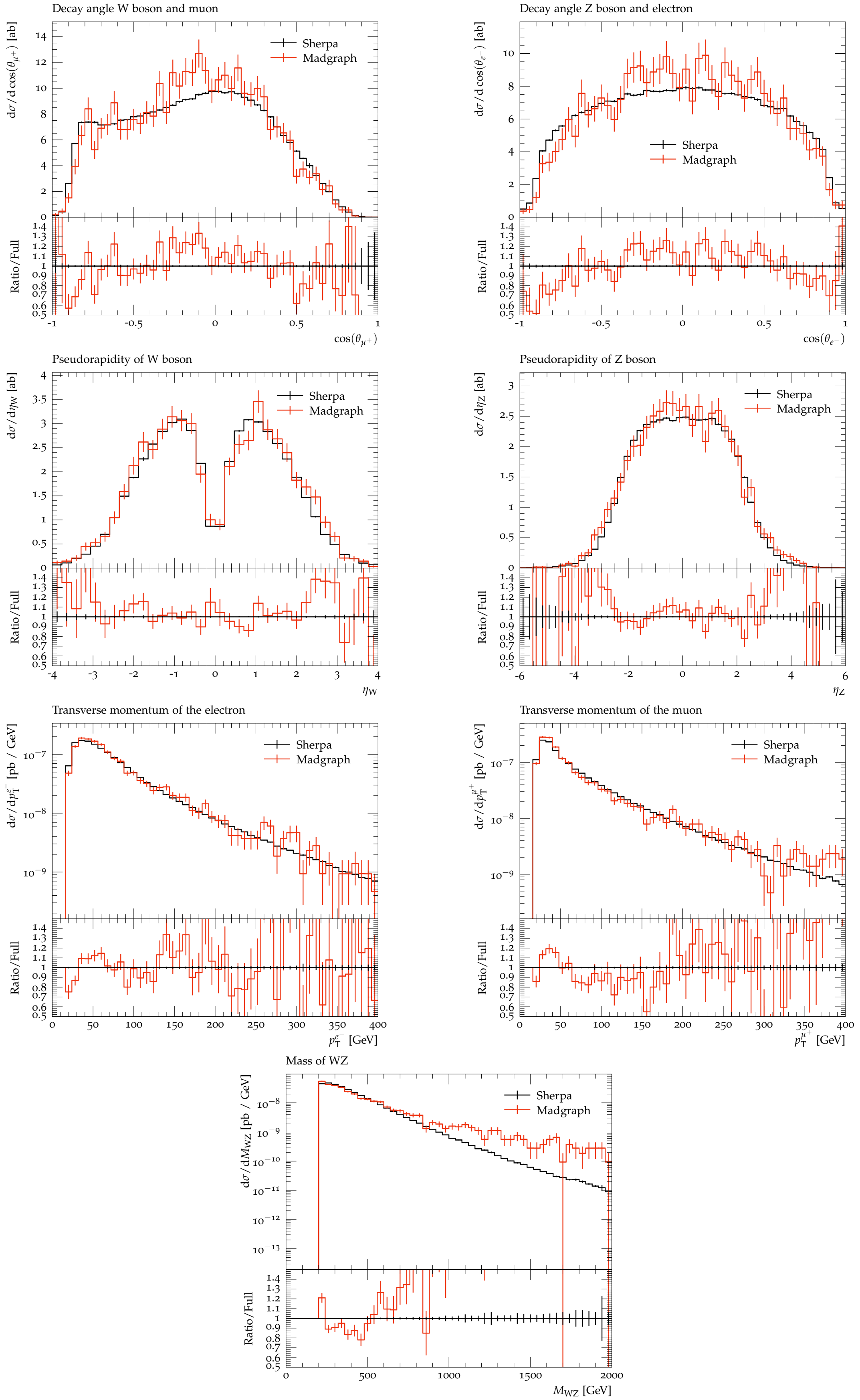

Figure A.1: Comparison of differential cross sections for a longitudinally polarized W^+ and Z boson between Sherpa and MadGraph

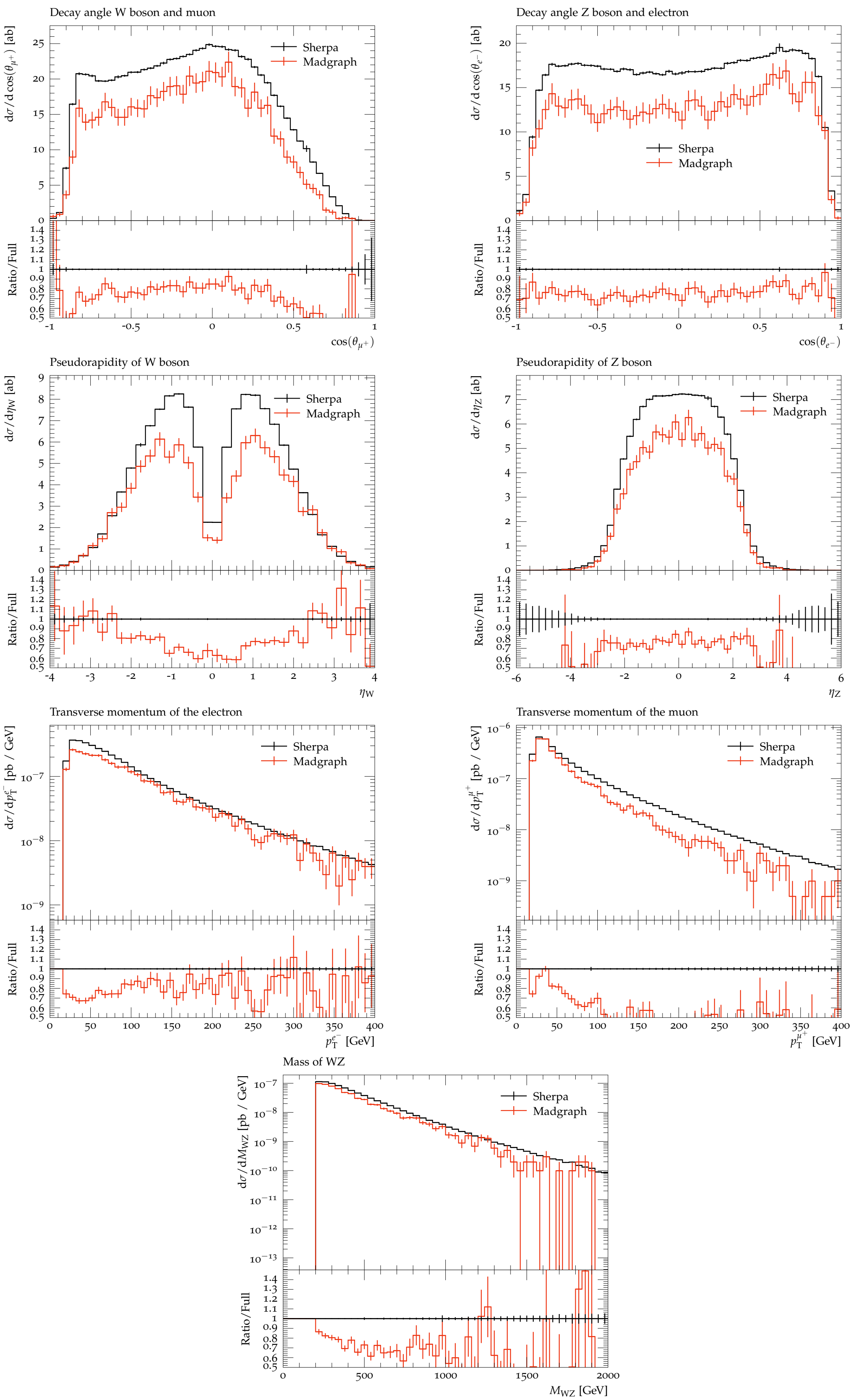

Figure A.2: Comparison of differential cross sections for a longitudinally polarized W^+ and a transverse polarized Z boson between Sherpa and MadGraph

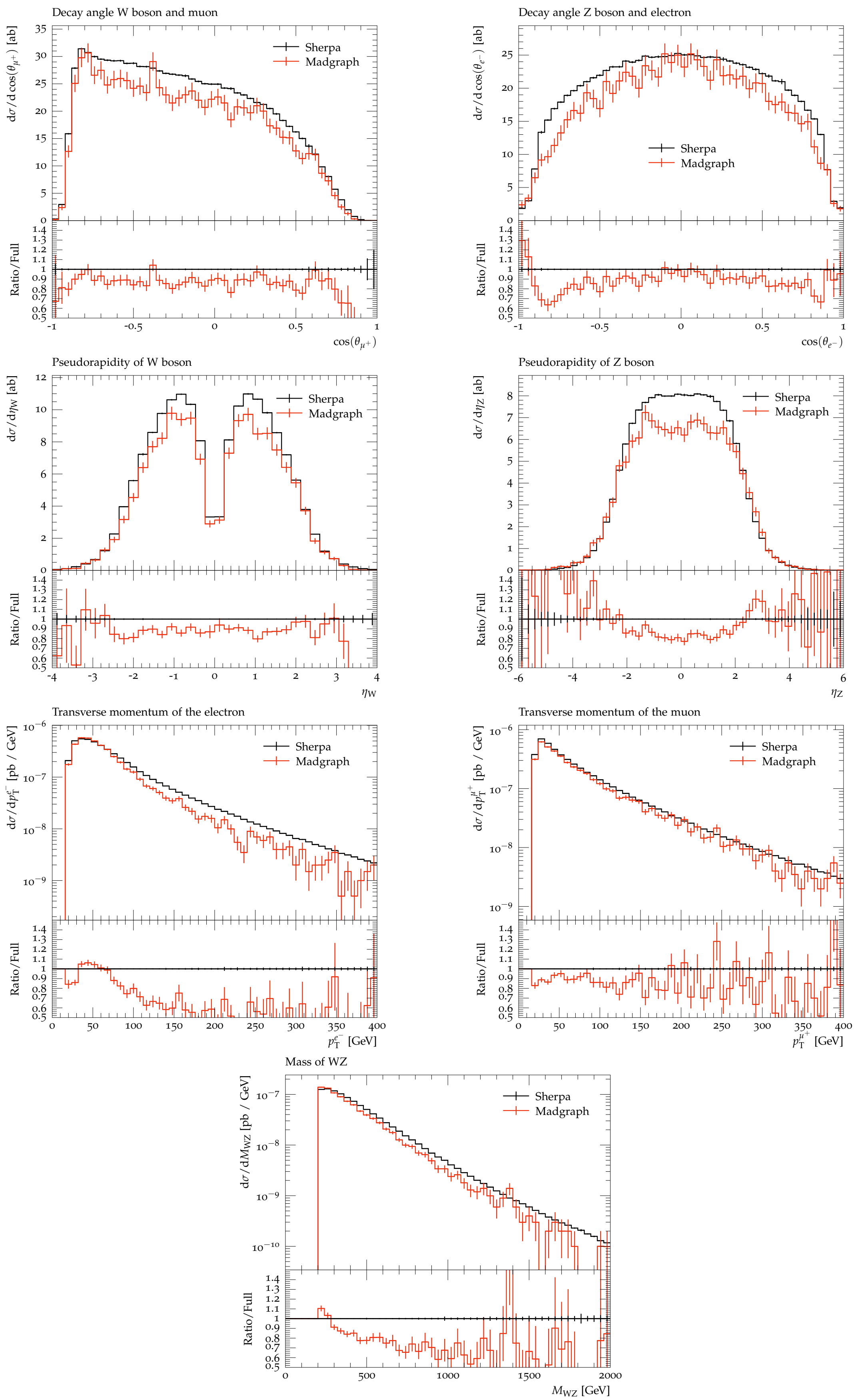

Figure A.3: Comparison of differential cross sections for a transverse polarized W^+ and a longitudinally polarized Z boson between SHERPA and MADGRAPH

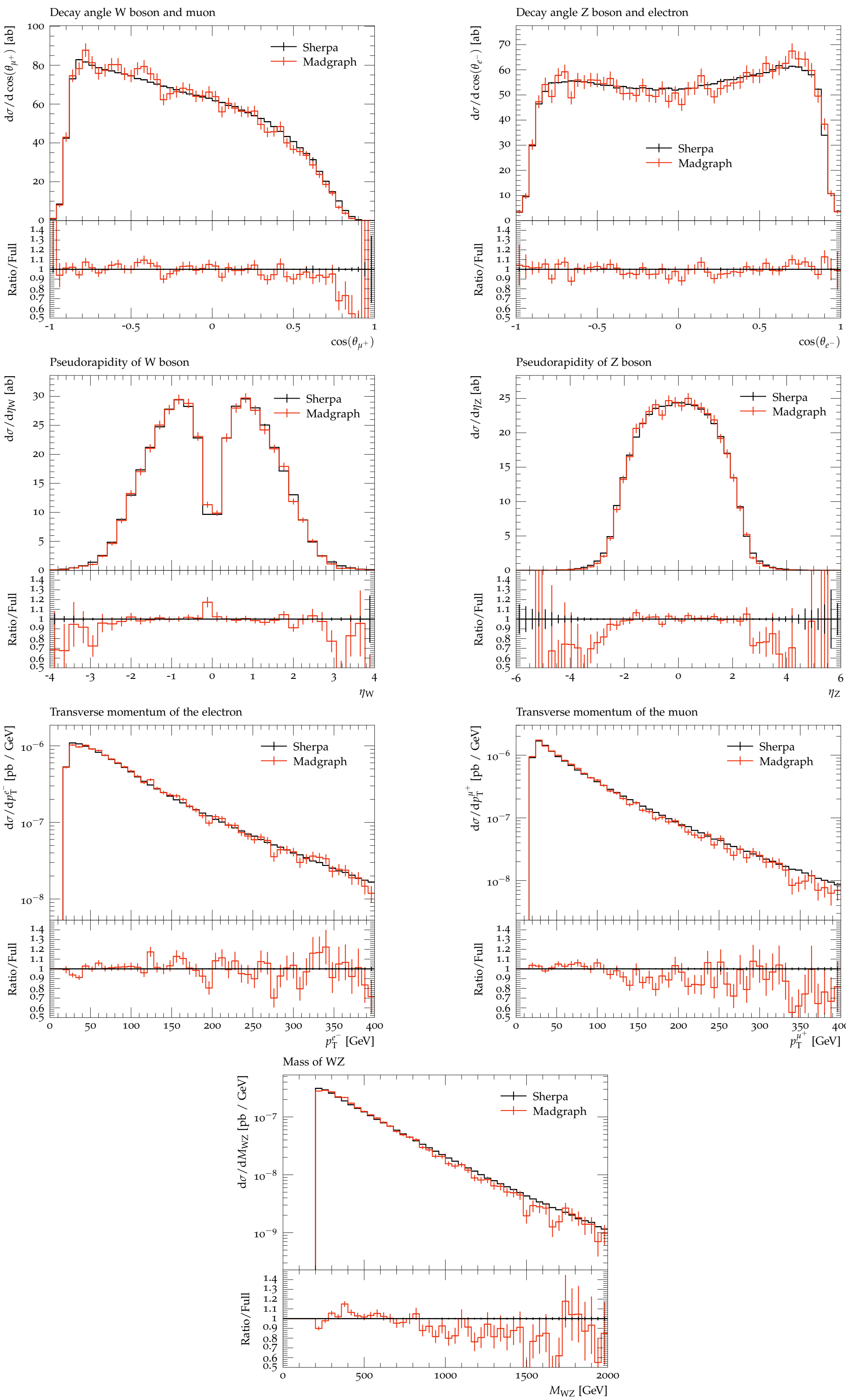

Figure A.4: Comparison of differential cross sections for a transverse polarized W^+ and Z boson between Sherpa and MadGraph

Bibliography

[1] Guido ALTARELLI. *The Standard Model of Particle Physics*. 2005. DOI: 10.48550/ARXIV.HEP-PH/0510281. URL: https://arxiv.org/abs/hep-ph/0510281.

[2] J. Alwall et al. "The automated computation of tree-level and next-to-leading order differential cross sections, and their matching to parton shower simulations." In: *Journal of High Energy Physics* 2014.7 (July 2014). DOI: 10.1007/jhep07(2014)079. URL: https://doi.org/10.1007%5C%2Fjhep07%5C%282014%5C%29079.

[3] Christian Autermann. "Experimental status of supersymmetry after the LHC Run-I." In: *Progress in Particle and Nuclear Physics* 90 (2016), pp. 125–155. ISSN: 0146-6410. DOI: https://doi.org/10.1016/j.ppnp.2016.06.001. URL: https://www.sciencedirect.com/science/article/pii/S0146641016300205.

[4] Julien Baglio and Le Duc Ninh. "Fiducial polarization observables in hadronic WZ production: a next-to-leading order QCDEW study." In: *Journal of High Energy Physics* 2019.4 (Apr. 2019). DOI: 10.1007/jhep04(2019)065. URL: https://doi.org/10.1007%5C%2Fjhep04%5C%282019%5C%29065.

[5] A. Ballestrero, E. Maina, and G. Pelliccioli. "Polarized vector boson scattering in the fully leptonic WZ and ZZ channels at the LHC." In: *Journal of High Energy Physics* 2019.9 (Sept. 2019). DOI: 10.1007/jhep09(2019)087. URL: https://arxiv.org/abs/1907.04722.

[6] D. Berdine, N. Kauer, and D. Rainwater. "Breakdown of the Narrow Width Approximation for New Physics." In: *Phys. Rev. Lett.* 99 (11 Sept. 2007), p. 111601. DOI: 10.1103/PhysRevLett.99.111601. URL: https://link.aps.org/doi/10.1103/PhysRevLett.99.111601.

[7] Christian Bierlich et al. *A comprehensive guide to the physics and usage of PYTHIA 8.3*. 2022. DOI: 10.48550/ARXIV.2203.11601. URL: https://arxiv.org/abs/2203.11601.

[8] Christian Bierlich et al. "Robust Independent Validation of Experiment and Theory: Rivet version 3." In: *SciPost Physics* 8.2 (Feb. 2020). DOI: 10.21468/scipostphys.8.2.026. URL: https://doi.org/10.21468%5C%2Fscipostphys.8.2.026.

[9] Carsten Bittrich. "Study of Polarization Fractions in the Scattering of Massive Gauge Bosons $W^{\pm}Z \rightarrow W^{\pm}Z$ with the ATLAS Detector at the Large Hadron Collider." Presented 2015. 2015. URL: https://cds.cern.ch/record/2014124.

[10] Enrico Bothmann et al. "Event Generation with Sherpa 2.2." In: *SciPost Phys.* 7.3 (2019), p. 034. DOI: 10.21468/SciPostPhys.7.3.034. arXiv: 1905.09127 [hep-ph].

[11] Andy Buckley et al. "General-purpose event generators for LHC physics." In: *Physics Reports* 504.5 (July 2011), pp. 145–233. DOI: 10.1016/j.physrep.2011.03.005. URL: https://doi.org/10.1016%5C%2Fj.physrep.2011.03.005.

[12] Andy Buckley et al. "LHAPDF6: parton density access in the LHC precision era." In: *The European Physical Journal C* 75.3 (Mar. 2015). DOI: 10.1140/epjc/s10052-015-3318-8. URL: https://doi.org/10.1140%5C%2Fepjc%5C%2Fs10052-015-3318-8.

[13] S. Dawson. *Introduction to Electroweak Symmetry Breaking.* 1999. DOI: 10.48550/ARXIV.HEP-PH/9901280. URL: https://arxiv.org/abs/hep-ph/9901280.

[14] Stefan Dittmaier. "Weylvan der Waerden formalism for helicity amplitudes of massive particles." In: *Physical Review D* 59.1 (Dec. 1998). DOI: 10.1103/physrevd.59.016007. URL: https://doi.org/10.1103%5C%2Fphysrevd.59.016007.

[15] F. Englert and R. Brout. "Broken Symmetry and the Mass of Gauge Vector Mesons." In: *Phys. Rev. Lett.* 13 (9 Aug. 1964), pp. 321–323. DOI: 10.1103/PhysRevLett.13.321. URL: https://link.aps.org/doi/10.1103/PhysRevLett.13.321.

[16] Lyndon Evans and Philip Bryant. "LHC Machine." In: *Journal of Instrumentation* 3.08 (Aug. 2008), S08001. DOI: 10.1088/1748-0221/3/08/S08001. URL: https://dx.doi.org/10.1088/1748-0221/3/08/S08001.

[17] Mareen Hoppe. "Polarized cross sections for vector boson production with Sherpa." In: (2022). URL: https://indico.cern.ch/event/1150707/contributions/5112606/.

[18] "Measurement of electroweak WZ boson production and search for new physics in WZ + two jets events in pp collisions at s=13TeV." In: *Physics Letters B* 795 (2019), pp. 281–307. ISSN: 0370-2693. DOI: https://doi.org/10.1016/j.physletb.2019.05.042. URL: https://www.sciencedirect.com/science/article/pii/S0370269319303636.

[19] Jan-Eric Nitschke. "Studies on polarization in the scattering of two vector bosons with the ATLAS experiment at the LHC." Presented 01 Nov 2019. 2019. URL: https://cds.cern.ch/record/2771952.

[20] "Observation of a new boson at a mass of 125 GeV with the CMS experiment at the LHC." In: *Physics Letters B* 716.1 (2012), pp. 30–61. ISSN: 0370-2693. DOI: https://doi.org/10.1016/j.physletb.2012.08.021. URL: https://www.sciencedirect.com/science/article/pii/S0370269312008581.

[21] "Observation of a new particle in the search for the Standard Model Higgs boson with the ATLAS detector at the LHC." In: *Physics Letters B* 716.1 (2012), pp. 1–29. ISSN: 0370-2693. DOI: https://doi.org/10.1016/j.physletb.2012.08.020. URL: https://www.sciencedirect.com/science/article/pii/S037026931200857X.

[22] P. J. E. Peebles and Bharat Ratra. "The cosmological constant and dark energy." In: *Rev. Mod. Phys.* 75 (2 Apr. 2003), pp. 559–606. DOI: 10.1103/RevModPhys.75.559. URL: https://link.aps.org/doi/10.1103/RevModPhys.75.559.

[23] *Standard Model Physics at the HL-LHC and HE-LHC.* 2019. DOI: 10.48550/ARXIV.1902.04070. URL: https://arxiv.org/abs/1902.04070.

[24] W. J. Stirling and E. Vryonidou. "Electroweak gauge boson polarisation at the LHC." In: *Journal of High Energy Physics* 2012.7 (July 2012). DOI: 10.1007/jhep07(2012)124. URL: https://doi.org/10.1007%5C%2Fjhep07%5C%282012%5C%29124.

[25] Sherpa Team. "Sherpa 3.0.0 Manual." In: (2022). URL: https://sherpa-team.gitlab.io/sherpa/master/index.html.

[26] Anna Sophie Tegetmeier. "Multivariate Analysis of Polarized Vector Boson Scattering of a W and Z Boson with the ATLAS Detector." Presented 2022. 2022. URL: http://cds.cern.ch/record/2842600.

[27] Mark Thomson. *Modern Particle Physics.* Cambridge University Press, 2013. DOI: 10.1017/CBO9781139525367.

Danksagung

Zunächst danke ich Dr. Frank Siegert, dass er mir die Möglichkeit gegeben hat, in seiner Arbeitsgruppe an diesem interessanten Thema zu forschen. Ein weiterer Dank richtet sich an Mareen Hoppe, die mich während dieser Bachelorarbeit betreut hat und immer Zeit für offene Fragen und Probleme gehabt hat. Des Weiteren möchte ich mich bei Anna Tegetmeier, Max Stange, Tim Herrmann, Erik Bachmann und Orcun Kolay bedanken, sie haben sich immer die Zeit genommen und mich jederzeit unterstützt. Ich bin dankbar für die stets herzliche Atmosphäre, die in dieser Arbeitsgruppe herrscht.
Ebenso möchte ich mich bei meinen Eltern, meiner Schwester und meinen Freunden bedanken, die mich während meines Studiums begleitet haben.

Erklärung

Hiermit erkläre ich, dass ich diese Arbeit im Rahmen der Betreuung am Institut für Kern- und Teilchenphysik ohne unzulässige Hilfe Dritter verfasst und alle Quellen als solche gekennzeichnet habe.

Tim Burghardt
Dresden, Dezember 2022